UNIVERSIDADE DE PASSO FUNDO
Graduate Program in Applied Computing

Master's Thesis

SIMULATING PEST AND DISEASE DAMAGE IN WHEAT PROCESS-BASED CROP MODELS

THIAGO BERTON FERREIRA

UPF

UNIVERSITY OF PASSO FUNDO
INSTITUTE OF EXACT SCIENCES AND GEOSCIENCES
GRADUATE PROGRAM IN APPLIED COMPUTING

SIMULATING PEST AND DISEASE DAMAGE IN WHEAT PROCESS-BASED CROP MODELS

Thiago Berton Ferreira

Thesis submitted to the University of Passo Fundo in partial fulfillment of the requirements for the degree of Master in Applied Computing.

Advisor: Prof. Dr. Willinghton Pavan

Passo Fundo
2021

CIP – Catalogação na Publicação

F383s Ferreira, Thiago Berton
Simulating pest and disease damage in wheat process-based crop models [electronic resouce] / Thiago Berton Ferreira. – 2021.
37 MB ; PDF.

Advisor: PhD. Willinghton Pavan.
Master's Thesis (Master in Applied Computing) – University of Passo Fundo, 2020.

1. Software engineering. 2. Agricultural informatics. 3. Simulation models. 4. Wheat – Disease and pest. I. Pavan, Willinghton, advisor. II. Title.

CDU: 631:004

Catalogação: Bibliotecária Juliana Langaro Silveira – CRB 10/2427

PPGCA
Programa de Pós-Graduação
em Computação Aplicada
Instituto de Ciências Exatas e Geociências | ICEG

MINUTE OF
ACADEMIC COURSE CONCLUSION WORK

THIAGO BERTON FERREIRA

On the twenty-three days of March two thousand and twenty-one, at 03:00 pm BRT, by online, through video conference, was held the public defense session of the Course Final Work “Simulating Pest and Disease Damage in Wheat Process-based Crop Models” authored by Thiago Berton Ferreira, academic of the Graduate Program in Applied Computing - PPGCA / UPF. According to Postgraduate Council's information and listed in the PPGCA Secretariat archives, the student fulfilled the requirements to submit his work to be evaluated. The examination board was composed by Dr. Willingthon Pavan (Advisor), Dr. Carlos Amaral Hölbig (UPF), Dr. Diego Noleto Luz Pequeno (CIMMYT - Mexico), PhD. José Maurício Cunha Fernandes (Embrapa Trigo), and PhD. Senthold Asseng (TUM - Germany). After the presentation and arguing, the examining board considered the candidate **APPROVED.** A period of up to forty-five (45) days, according to the Rules of the PPGCA, was granted for the academic to submit the final writing to the Postgraduate Council to make the necessary referrals for the issuance of Master in Applied Computing diploma. To record, this minute was drawn up, signed by the examination board members and the PPGCA Coordinator.

DocuSigned by:
WILLINGTHON PAVAN
4810E0667FBA4A2...
Prof. Dr. Willingthon Pavan – UPF
Examining Committee President
(Advisor)

DocuSigned by:
26790BBACB944B7...
Prof. Dr. Carlos Amaral Hölbig – UPF
(Internal Examinator)

DocuSigned by:
E4AA4DF364004DB...
Dr. Diego Noleto Luz Pequeno – CIMMYT (Mexico)
(External Examinator)

DocuSigned by:
792F0255B0C94A6...
PhD. José Maurício Cunha Fernandes – Embrapa Trigo
(External Examinator)

DocuSigned by:
Senthold Asseng
61A26994905841A...
PhD. Senthold Asseng – TUM (Germany)
(External Examinator)

DocuSigned by:
26790BBACB944B7...
Prof. Dr. Carlos Amaral Hölbig
PPGCA Coordinator

SIMULAÇÃO DE PRAGAS EM MODELOS DE CRESCIMENTO DE TRIGO

RESUMO

Pragas e doenças são conhecidas por causar danos às lavouras de trigo (*Triticum aestivum* L.) e reduzir o desenvolvimento das mesmas. Esses estresses bióticos estão frequentemente, ou sempre, associados à perda de safras que ameaçam a produção de trigo em todo o mundo. Modelos de doenças de plantas podem ajudar a estimar o impacto de pragas e doenças no crescimento da cultura, no entanto, isso ainda é um desafio, pois este impacto é pouco reconhecido como um dos principais fatores que limitam a produtividade. O objetivo deste projeto foi desenvolver e testar um método para simular pragas e doenças do trigo por meio do modelo de simulação de trigo CSM-NWheat e estudar a redução no desenvolvimento da cultura e da produtividade devido ao estresse biótico. Este estudo também se comprometeu a desenvolver uma abordagem dinâmica usando uma interface MPI (Message Passing Interface) para acoplar o mesmo modelo de crescimento do trigo com vários modelos de doenças, a fim de analisar os efeitos prejudiciais do oídio (*Blumeria graminis f. Sp. Tritici*), mancha marrom (*Pyrenophora tritici-repentis*) e giberela (*Gibberella zeae*) na produção de trigo. Com a implementação observou-se um aumento na exatidão do modelo do trigo onde o rendimento e o índice de área foliar (AF) simulado obtiveram valores mais próximos a realidade. O CSM-NWheat agora pode estimar os danos no índice de área foliar, massa foliar, massa do caule, massa da raiz, massa da semente, AF necrótica, assimilados e a planta como um todo. A estratégia multimodelo também mostrou um efeito positivo na simulação de perdas de safra devido à infecção fúngica e um novo método de acoplamento para modelos de trigo.

Palavras-Chave: Estresses bióticos, crescimento do trigo, DSSAT, modelos de doenças de plantas.

SIMULATING PEST AND DISEASE DAMAGE IN WHEAT PROCESS-BASED CROP MODELS

ABSTRACT

Pests and diseases are known for causing damage to wheat (*Triticum aestivum* L.) crops and reduce plant development. These biotic stresses are often, or always, associated with crop loss which threatens wheat production and security worldwide. Plant disease models can help estimate the impact of pests and diseases on crop growth however, this is still a challenge since it is poorly recognized as one of the main factors that limit yield. The objective of this project was to develop and test a method to simulate wheat pests and diseases through the CSM-NWheat wheat model and study the reduction in crop development and yield due to biotic stress. This study also compromised to develop a dynamic approach using an MPI (Message Passing Interface) interface to couple the same wheat growth model with multiple disease models to analyze the damaging effects of powdery mildew (*Blumeria graminis f. sp. tritici*), tan spot (*Pyrenophora tritici-repentis*) and fusarium head blight (*Gibberella zeae*) on wheat yield. The newly pest-coupled CSM-NWheat can now estimate damage on leaf area index (LAI), leaf mass, stem mass, root mass, seed mass, necrotic leaf area, assimilates, and the whole/complete plant. Case studies demonstrated the model's capability of simulating losses due to pest and disease infection similarly to the field observed data. Additionally, the multi-model strategy presented a positive effect on simulating crop losses due to fungal infection as well as a new coupling method for wheat models. This model extension enhanced the accuracy of the wheat model and, compared with the field data, the simulated yield and LAI were improved to a great extent.

Keywords: Biotic stresses, wheat growth, DSSAT, plant disease models.

LIST OF FIGURES

LIST OF TABLES

CONTENTS

1. INTRODUCTION

Wheat (*Triticum aestivum* L.) provides nearly 20% of the daily calories and protein to the global population. It is one of the world's most consumed cereals and a major staple food in many countries [1]. With the crescent growth of the population worldwide, the need to enhance wheat production and its security as a food source raise exponentially. Consequently, this requires methods to help farmers maximize crop yield and minimize loss. Crop pathogens and pests are estimated to be responsible for 20% to 40% of the worldwide agricultural production loss and 10.1 to 28.1% of global production losses of wheat crops [2]. The ever-growing necessity of maximizing crop yield also brings up the necessity to control and reduce the pest incidence. Modeling tools such as crop growth models and pest models can supply this need and provide means to increase crop production. However, measuring the impact of plant pests and diseases on plant growth and development is currently an important and, at the same time, poorly studied research question within the crop modeling community [3, 4, 5].

In the early 1980's, pest and disease frameworks started to be developed as attempts to quantify the effects of pests and diseases on crop performance [6]. Along with, crop simulation models were designed to predict crop growth using two modeling approaches: the empirical, regression models that describes effects only at the level of observation; and the mechanistic, physiological models capable of explaining the observed growth rates in relation to the environmental factors [7]. Mechanistic models were the underlying method which crop models started to be coupled with pest models and/or assess pest management [8, 9].

The representation of damaging effects due to pests and diseases infection on crop growth can be given in several levels through functions for pest population dynamics and disease life cycle, for example. Boote [10] defined seven categories which pest damage can affect the carbon flow processes in crop models based on the types of damage these pests and diseases do: stand reducer, photosynthetic rate reducer, leaf senescence accelerator, light stealer, assimilate sapper, tissue eater or consumer, and turgor reducer. These damage mechanisms serve as a general method to incorporate the impact of pests and diseases into crop models. Based on this principles, pest coupling points were incorporated inside the Cropping System Model (CSM) of the Decision Support System for Agrotechnology Transfer (DSSAT) [11, 12, 13] which eventually led to the creation of a pest module (PEST) [14]. Although some mechanistic methods were created to simulate damage on wheat leaf area index (LAI) and grain yield [15, 16, 17], the account for pest and disease are still missing in many wheat models, this includes the wheat models within the DSSAT platform (CROPSIM-Wheat [18] and NWheat [19]).

The main objective of this thesis is to expand the PEST module inside DSSAT through the development of coupling points and pest subroutines inside the CSM-NWheat, a wheat crop growth model, to simulate and account the pest and disease damaging effects on wheat crops. Additionally, develop fungal disease models to simulate the disease cycle of powdery mildew (*Blumeria graminis f. sp. tritici*), tan spot (*Pyrenophora tritici-repentis*) and fusarium head blight (*Gibberella zeae*) and estimate the effects on wheat growth and yield. This work represents a new method to predict disease effects on crops and also enhance the decision support capability by providing useful production predictions in a real farm conditions.

The present work was divided into chapters based on two papers each as a chapter detailing the development of this project. Chapter 2 gives a brief overview of the agricultural pests and background on crop and pest modeling. Chapter 3 discuss the implementation of pest and disease coupling points inside the DSSAT CSM-NWheat to allow the damage estimation of pest and pathogens on wheat crops. This stands as one of the first wheat model capable of estimating pest damage during crop growth simulation. The Chapter 4, details the development of a multiple disease modeling approach, using the previous developed coupling points and a MPI interface, to simulate the effects of multiple pests in a wheat crop. Chapter 5 presents a summarization of this project and future work.

2. BACKGROUND

2.1 AGRICULTURAL PESTS AND DISEASES

Plant pests and diseases are one of the main factors that limit crop production and threaten food security worldwide. The spread of pests and diseases increased rapidly across crop growing areas in recent years. Globalization, climate change and the rise on food demand are factors that may have collaborated to the increase of pest and disease pressure on agricultural systems [20], impacting their behaviour and distribution.

Transboundary plant pests and diseases such as wheat and rice blast, caused by fungal pathogens, *Magnaporthe oryzae triticum* (MoT) and *Magnaporthe oryzae triticum* are destructive diseases that affect grain development of wheat and rice [21]. Rainy and humid weather conditions are critical for infection since these pathogens require free moisture on the plant surface to penetrate the host cells [22] (Figure 1). Both MoT and *Magnaporthe oryzae* pathogens are hemibiotrophic, organisms that infect living tissue for some time and, afterward, live on dead tissue [23]. The life cycle of these diseases starts when the ascospore pierce the host cuticle and the fungus starts to grow within the plant cells. These eventually lead to disease lesions and, when high humidity conditions are reached, the fungus sporulates and spreads to adjacent plants through the wind or water droplets. Later, as the lesions become apparent, the fungus starts its necrotrophic phase promoting plant cell death [24].

Figure 1. Wheat field conditions after rainfall favoring plant-pathogenic fungus infection

Other fungal diseases caused by some species of *Fusarium* produce mycotoxins to enter the seed structure causing tissue necrosis inside the kernels. This mycotoxins are used to disable plant defense mechanisms while killing the host cells. For example, the deoxynivalenol (DON) is the main mycotoxin produced by *Fusarium gramenearum* [25] and it is toxic to humans and animals [26].

Insect pests such as the *Helicoverpa Zea* and *Helicoverpa Armigera* are also extremely harmful to crop production. The development of these insects depend strictly on temperature, rainfall and the food source available [20] whereas the larvae can rear on a

large variety of plants. *Helicoverpa Zea*, popular known as corn earworm, is a major problem in North America and can be found in crops of soybean, cotton, tomatoes and others. *Helicoverpa Armigera*, also known as cotton bollworm, is a moth easily found in Africa, Europe and Asia and has developed resistance for a wide range of insecticides [27].

2.2 WHEAT FUNGAL PATHOGENS

Wheat is commonly attacked by fungal pathogens such as rust diseases, leaf spot diseases and others [28]. This parasites attack and destroy plant cells and can have a huge impact on the wheat production in the world. A clear example of disaster caused by biotic stresses is the major outbreak of wheat blast in Bangladesh, a disease that prior to this event was only found in wheat crops of South America, which resulted in a 51% yield loss in 2016 [29, 21]. Ceresini et al. [30] assumed that the wheat blast outbreak happened through wheat grain trading from Brazil to Bangladesh.

Pathogens such as powdery mildew (*Blumeria graminis f. sp. tritici*), tan spot (*Pyrenophora tritici-repentis*) and fusarium head blight (*Gibberella zeae*) have different aspects and conditions for infection. For example, powdery mildew disease is a biotrophic parasite that feeds only on living plant stem and leaves, producing white powdery spots that reduce the efficiency of photosynthesis [31]. The spores infect the host cells through penetration pegs causing the plant to shunt resources to the fungus. Its optimal environmental conditions for germination is with temperature between 15 and 25 ℃ with relative humidity higher than 85%. On the other hand, necrotrophic parasites such as tan spot and fusarium head blight (FHB) survive on dead tissues and do not necessarily need a living host plant. These diseases infects wheat plants under warm and humid environments and induce plant chlorosis and necrosis symptoms. Tan spot infects the wheat leaves and the fungus destroys the living tissue expanding into lens-shaped lesions with a brown spot in the center and yellow borders [32]. FHB infects the wheat grains resulting in kernel weight reduction, quality deterioration and mycotoxin contamination. This mycotoxin named Deoxynivalenol or DON is toxic not only to humans but also to livestock animals [25].

Plant breeding has been largely used in order to produce cultivar with high resistance against certain diseases and reduce disease impact [33] but, there are no wheat cultivars resistant to multiple diseases and all races. Integrated pest management has also shown positive effects against crop pests and diseases in general. However, the gap between potential and attained yield still is substantial. For this reason, crop models coupled with pest and disease models can help reduce this yield loss.

2.3 CROP MODELING

As agricultural systems become more complex and intense, the demand for better means of environmental control within planting areas increases. Crop simulation models (CSM) can help supply a basis for improving soil and crop management as well as crop production. These simulation models are employed as a way to describe and predict crop growth, taking into consideration factors such as weather conditions, soil type, crop management, and others. Platforms for crop growth simulation such as the Decision Support System for Agrotechnology Transfer (DSSAT) and the Agricultural Production Systems sIMulator (APSIM) are frameworks used to simulate biophysical processes in farming systems for a diverse range of crops [14, 34].

2.3.1 Agricultural Production Systems sIMulator

Agricultural Production Systems sIMulator (APSIM) is a suite of models capable of simulating of complex agricultural systems such as soil, crop, tree, pasture and livestock. The framework was originally developed using FORTRAN in early 90's. Recently, the APISM initiative started bulding the next generation [35] of APSIM using GTK for creating a new cross-platform application. However, APSIM currently does not incorporate pests and diseases damage during crop growth simulation.

2.3.2 Decision Support System for Agrotechnology Transfer

The Decision Support System for Agrotechnology Transfer (DSSAT) platform comprises more than forty-two crop models that simulate plant development, taking into account multiple variables, like soil type, weather, genetics, crop management, and others [36, 14]. It provides tools to assist the user in preparing the different input files required to run a model, conduct analysis of the simulation outputs, and compare them with the observed data. The Cropping System Model (CSM) of DSSAT simulates crop growth, biomass development and yield as a function of the environment dynamics such as weather, soil and plant interactions. The DSSAT platform also has a built-in pest module called PEST, which communicates with some crop growth models.

2.3.2.1 DSSAT Pest Module

The DSSAT PEST module interacts with the crop model to estimate the effects of pests and pathogens. Although DSSAT has a large variety of crops, the PEST module only communicates with CROPGRO family of models [37] and the CERES models: Maize,

sorghum, and millet [38]. The CERES-Wheat model also had a single coupling point added to the structure to simulate impact of *septoria tritici blotch* (STB) on wheat leaf area index and yield [17]. The current PEST module started as a set of independent disease/pest modules and represent a collaborative work made over the past 40 years. The system was designed to simulate the likely effects of pests and diseases on crop growth through linear interpolation between scouting reports. According to pest population and feeding rate, the values are then converted into daily damage rates, which affect one or more specific plant parts and, consequently, the crop yield.

The simulation of pest damage using the PEST module requires two input files, a pest coefficients file (fileP) and time series data file (fileT). The fileP defines which coupling points the pest will act upon and the respectively damage pattern [12]. Therefore, DSSAT's PEST module can estimate the pest damage rate and the specific units (e.g. m^2 m^{-2}, g m^{-2}). On Figure 2 is presented an example of pest coefficient file for soybean (SBGRO047.PST).

Figure 2. Example of pest coefficient file for soybean SBGRO047.PST (http://github.com/DSSAT/dssat-csm-os).

LN	PID	PNAME	PCTID	PCPID	PDCF1		UNITS	SOURCE
01	CEW6	Corn Earworm	2	LAD	1.00000000	0.0000	no./larva/d	Batchelor et al., 1989
99	CCCC	Corn Earworm	4	SDNL	2.50000000	0.0000	no./larva/d	Batchelor et al., 1989
				LAD	0.00505000	0.0000	no./larva/d	Batchelor et al., 1989
02	VBC5	5 Instar Velvetbean	1	LAD	0.00081000	0.0000	m2/larva/d	Reid, 1975
				SDNL	2.50000000	0.0000	no./larva/d	Szmedra et al., 1988
				LAD	0.00505000	0.0000	m2/larva/d	Szmedra et al., 1988
03	VBC6	6 Instar Velvetbean	1	LAD	0.00144000	0.0000	m2/larva/d	Reid, 1975
04	SL4	Soybean Looper	1	LAD	0.00044000	0.0000	m2/larva/d	Reid and Green, 1975
05	SL5	Soybean Looper	1	LAD	0.00071000	0.0000	m2/larva/d	Reid and Green, 1975
06	SL6	Soybean Looper	1	LAD	0.00124000	0.0000	m2/larva/d	Reid and Green, 1975
07	SGSB	Stinkbug	4	SDNS	15.0000000	0.0000	no./m2/d	Batchelor et al., 1989
				SDNM	5.00000000	0.0000	no./m2/d	Batchelor et al., 1989
08	FAW	Fall Armyworm	1	LMD	2.00000000	0.0000	g/larva/day	estimated
09	RTWM	rootworm	1	RLV	1.00000000	0.0000	cm/cm2/lar/d	estimated
10	PCLA	Obs.% defoliation	2	LAD	1.00000000	0.0000	%	estimated
11	PSTM	Obs.% Stem damage	2	SMD	1.00000000	0.0000	%	estimated
12	PDLA	% Diseased Leaf Area	3	PDLA	1.00000000	0.0000	%/day	estimated
13	PRP	% Reduction in Photo	3	ASM	1.00000000	0.0000	%/day	estimated
14	PLAI	% daily LAI dest.	3	LAD	1.00000000	0.0000	%/day	estimated
15	PLM	% daily Leaf Mass	3	LMD	1.00000000	0.0000	%/day	estimated
16	PWP	% Whole Plants	3	WPD	1.00000000	0.0000	%/day	estimated
17	PSDN	% All Seed Dest.	3	SDNL	1.00000000	0.0000	%/day	estimated
				SDNS	1.00000000	0.0000	%/day	estimated
				SDNM	1.00000000	0.0000	%/day	estimated
18	PSHN	% All Shell Dest.	3	SHNL	1.00000000	0.0000	%/day	estimated
				SHNS	1.00000000	0.0000	%/day	estimated
				SHNM	1.00000000	0.0000	%/day	estimated
19	PPDN	% All Pod Dest.	3	PPDN	1.00000000	0.0000	%/day	estimated
20	PRTM	% Root mass dest.	3	RMD	1.00000000	0.0000	%/day	estimated
23	MOW	Top weight left.	3	TOPWT	1.00000000	0.0000	kg/ha top weight left	

Pest Number (LN), pest abbreviation (PID), pest name (PNAME) are pest identifiers. Damage characterization method (PCTID) indicates the damage method. Damage characterization method (PCPID) specify the affected coupling point(s). Feeding rate coefficient (PDCF1) describes the damage caused by the pest to the crop. Units of feeding rate (UNITS) characterize the pest damage unit. Source column indicates where the values and the information were collected.

The field-specific file with observed data about crop development (fileT) is used as data comparison of the measured and simulated results over the course of time [38]. However, when the pest factor is detailed in the experiment, fileT describes the different pest level or damage observed throughout the entire season. The PEST module then uses

the pest observed data from the trial to estimate pest damage. A linear interpolation method is applied to compute pest and/or disease damage between entries in the fileT time series [39]. Figure 3 is an example of soybean fileT (UFGA7802.SBT).

Figure 3. Example of time series data file for soybean UFGA7802.SBT (http://github.com/DSSAT/dssat-csm-od).

@TRNO	DATE	LAID	SWAD	GWAD	LWAD	CWAD	PWAD	SHAD	SH%D	SLAD	HIAD	CEW6
1	78194	.89	178	0.	266	444	0.	0.	0.00	334.6	0.0	0.0
1	78201	1.28	300	0.	366	667	0.	0.	0.00	349.7	0.0	0.0
1	78208	1.91	551	0.	656	1207	0.	0.	0.00	291.2	0.0	0.0
1	78215	2.86	943	0.	843	1786	0.	0.	0.00	339.3	0.0	0.0
1	78222	4.17	1561	0.	1187	2748	0.	0.	0.00	351.3	0.0	0.0
1	78229	3.90	1956	0.	1204	3160	0.	0.	0.00	323.9	0.0	0.0
1	78236	4.66	2947	0.	1723	4792	123	123	0.00	270.5	0.0	0.0
1	78243	4.47	3144	0.	1772	5224	308	308	0.00	252.3	0.0	0.0
1	78250	4.44	3303	182	1631	5740	805	623	22.60	272.2	0.030	0.0
1	78257	3.99	3326	754	1568	6507	1613	859	46.75	254.5	0.116	0.0
1	78264	4.67	3657	1912	1769	8586	3161	1249	60.49	264.0	0.222	0.0
1	78271	2.83	2732	2223	1180	7144	3232	1009	68.78	239.8	0.311	0.0
1	78278	2.09	2515	2730	858.0	7136	3763	1033	72.55	243.6	0.383	0.0
1	78285	.47	1851	2913	170.0	5866	3845	932	75.76	276.5	0.497	0.0
1	78292	.09	2064	3169	34.0	6270	4172	1003	75.96	264.7	0.505	0.0
2	78194	.75	160	0.	244	405	0.	0.	0.00	307.4	0.0	0.0
2	78201	1.08	251	0.	311	563	0.	0.	0.00	347.3	0.0	0.0
2	78208	1.81	535	0.	626	1161	0.	0.	0.00	289.1	0.0	0.0
2	78215	3.29	1080	0.	974	2054	0.	0.	0.00	337.8	0.0	0.0
2	78222	4.38	1663	0.	1261	2923	0.	0.	0.00	347.3	0.0	0.0
2	78229	4.30	2083	0.	1392	3475	0.	0.	0.00	308.9	0.0	0.0
2	78236	4.21	2556	0.	1517	4184	112	112	0.00	277.5	0.0	0.0
2	78243	4.50	2673	0.	1439	4431	319	319	0.00	312.7	0.0	0.0
2	78250	2.09	1998	42	838	3104	268	226	15.67	249.4	0.014	0.0
2	78257	3.24	2650	253	1220	4530	661	408	38.28	265.6	0.056	0.0
2	78264	2.30	2609	471	931	4440	901	430	52.28	247.0	0.106	0.0
2	78271	1.14	2113	775	498	3812	1200	425	64.58	228.9	0.203	0.0
2	78278	.85	1905	782	371	3398	1122	340	69.70	229.1	0.230	0.0
2	78285	.53	1922	1149	236	3732	1574	425	73.00	224.5	0.308	0.0
2	78292	.07	1590	1206	30	3250	1630	424	73.99	233.3	0.371	0.0
3	78194	.89	178	0.	266	444	0.	0.	0.00	334.6	0.0	0.0
3	78201	1.28	300	0.	366	667	0.	0.	0.00	349.7	0.0	0.0
3	78208	1.91	551	0.	656	1207	0.	0.	0.00	291.2	0.0	0.0
3	78215	2.86	943	0.	843	1786	0.	0.	0.00	339.3	0.0	0.0
3	78222	4.17	1561	0.	1187	2748	0.	0.	0.00	351.3	0.0	0.0
3	78229	3.90	1956	0.	1204	3160	0.	0.	0.00	323.9	0.0	0.5
3	78236	4.66	2947	0.	1723	4792	123	123	0.00	270.5	0.0	1.0
3	78243	4.47	3144	0.	1772	5224	308	308	0.00	252.3	0.0	2.5
3	78250	4.44	3303	182	1631	5740	805	623	22.60	272.2	0.030	5.5
3	78257	3.99	3326	754	1568	6507	1613	859	46.75	254.5	0.116	11.1
3	78264	4.67	3657	1912	1769	8586	3161	1249	60.49	264.0	0.222	14.1
3	78271	2.83	2732	2223	1180	7144	3232	1009	68.78	239.8	0.311	13.1
3	78278	2.09	2515	2730	858	7136	3763	1033	72.55	243.6	0.383	0.5
3	78285	.47	1851	2913	170	5866	3845	932	75.76	276.5	0.497	0.8
3	78292	.09	2064	3169	34	6270	4172	1003	75.96	264.7	0.505	0.9
4	78194	.75	160	0.	244	405	0.	0.	0.00	307.4	0.0	0.0
4	78201	1.08	251	0.	311	563	0.	0.	0.00	347.3	0.0	0.0
4	78208	1.81	535	0.	626	1161	0.	0.	0.00	289.1	0.0	0.0
4	78215	3.29	1080	0.	974	2054	0.	0.	0.00	337.8	0.0	0.0
4	78222	4.38	1663	0.	1261	2923	0.	0.	0.00	347.3	0.0	0.0
4	78229	4.30	2083	0.	1392	3475	0.	0.	0.00	308.9	0.0	0.5
4	78236	4.21	2556	0.	1517	4184	112	112	0.00	277.5	0.0	1.0

(1) TRNO - Treatment number, (2) DATE - Date observed (first two digits represent the year and last three the day of the year), (3) LAID - Leaf Area Index, (4) SWAD - Stem dry weight (kg/ha), (5) GWAD - Grain dry weight (kg/ha), (6) LWAD - Leaf dry weight (kg/ha), (7) CWAD - Crop dry weight (kg/ha), (8) PWAD Pot weight (kg/ha), (9) SHAD - Shell weight (kg/ha), (10) SH%D - Shelling percentage (seed wt/pod wt*100), (11) SLAD - Specific leaf area (cm^2/g), (12) HIAD - Harvest index (grain/top), (13) CEW6 - 6th instar corn earworm (*Helicoverpa Zea*).

The pest coupling points link the crop growth model with a pests or diseases model. This communication allows estimating the damage caused by pests or diseases daily and the respective effect on crop growth and development. Four pre-determined types of damage can be selected:

- Daily absolute damage rate (1) - express damage according to the pest population and their feeding rates.

- Percent observed damage rate (2) - useful when the exact damage rate is not known. Turns possible the comparison between a control treatment with a scientific treatment to obtain the percentage difference of leaf mass between plots, for example.
- Daily percent damage rate (3) - assigned when damage is expressed in daily percent loss. For example, the daily percentage of leaf loss due to defoliation.
- Daily absolute damage rate with pest competition and food preference effects (4) - used when there is food competition between pests or the pest causes damage to more than one coupling point [40].

These damage types can then be applied to a specific plant part of the plant as a whole. For example, the CROPGRO model includes twenty-three coupling points which pest damage can affect the simulated leaf area index (LAI), leaf mass, stem mass, root mass, seed mass (small, large, and mature sizes), shell, the whole/complete plant, assimilates, necrotic LAI, pod number, and vegetative nodes. All coupling points are presented in Table 1 as well as the respective units, available damage method, and the ID. More details of this pest coupling approach can be found on the DSSAT v4.5 Crop Model Documentation Vol. 4 [39].

Table 1. Coupling points and damage types used in CROPGRO crop models (Adapted from DSSAT v4.5 Crop Model Documentation)[41]

.

Coupling points	Units	Available Damage Type	Coupling Point ID (PCPID)
Leaf area index	$m^2 m^{-2}$	1,2,3,4	'LAD'
Leaf mass	$g\ m^{-2}$	1,2,3,4	'LMD'
Stem mass	$g\ m^{-2}$	1,2,3,4	'SMD'
Root mass	$g\ m^{-2}$	1,3,4	'RMD'
Root length	$cm\ root/cm^{-2}\ soil$	1,3,4	'RLF'
Root length density	$cm\ root/cm^{-3}\ soil$	1,3,4	'RLV'
Small seed number	$no.m^{-2}$	1,3,4	'SDNS'
Large seed number	$no.m^{-2}$	1,3,4	'SDNL'
Mature seed number	$no.m^{2}$	1,3,4	'SDNM'
Small seed mass	$g\ m^{-2}$	1,3,4	'SDMS'
Large seed mass	$g\ m^{-2}$	1,3,4	'SDML'
Mature seed mass	$g\ m^{-2}$	1,3,4	'SDMM'
Small shell number	$no.m^{-2}$	1,3,4	'SHNS'
Large shell number	$no.m^{-2}$	1,3,4	'SHNL'
Mature shell number	$no.m^{-2}$	1,3,4	'SHNM'
Small shell mass	$g\ m^{-2}$	1,3,4	'SHMS'
Large shell mass	$g\ m^{-2}$	1,3,4	'SHML'
Mature shell mass	$g\ m^{-2}$	1,3,4	'SHMM'
Whole plant	$no.m^{-2}$	1,3	'WPD'
Assimilate	$g\ m^{-2}$	1,3	'ASM'
Necrotic leaf area index	$cm^2\ cm^{-2}$	1,3,4	'PDLA'
Pod numbers	$\%/day$	3	'PPDN'
Vegetative nodes	$no.nodes$	1,3,4	'VSTG'

2.3.3 Wheat Pest Models

Although the current advances in coupling crop and pest modules, most wheat simulation models still do not account for pests and diseases' damage. Some previous studies, a model named WHEATPEST was developed to estimate the impact of specific pests on wheat yield through mean temperature and solar radiation, and an array of driving functions and parameters to simulate production and daily injuries caused by the pest to simulate the effects on yield loss [15]. A rust model developed in DYMEX population-modeling platform was coupled with the Agricultural Production Systems Simulator (APSIM) in order to estimate the impact of wheat rust on the green leaf area [4]. Savary et al. [42] developed a generic wheat disease model (EPIWHEAT) for estimating specifically the potential epidemics caused by leaf pathogens of wheat. The climate driven model divides the disease progression in the host tissue into four categories: healthy, latent, infectious and removed. These categories detail the monocycle of the disease considering also the expansion rate of the lesions. In the same year, Caubel et al. [43] coupled the MILA, a model for simulat-

ing airborne fungal pathogens responsible for foliar diseases, with a wheat version of STICS (Simulateur mulTIdisciplinaire pour les Cultures Standard) crop model [44] for estimating the effects of leaf rust based on leaf wetness and temperature. The coupled model measured the climate change effects on three different scenarios (2.6, 4.5 and 8.5 RCP - Representative Concentration Pathway), reducing the plant photosynthesis according to the number of spores and lesions in the leaf surface. An earth system model also was used to predict the climate change impacts on the spread potential of wheat stem rust [45]. The model estimated the emission and transport of the urediniospores for the modern (2000) and future (2100) following the RCP8.5 scenario and driven by the temperature, light and leaf wetness at the deposition area. Bregaglio et al. [46] incorporated into five different wheat models a pest damage mechanism tosimulate four major wheat diseases (brown and yellow rust, septoria triticiblotch and powdery mildew). Within the DSSAT platform and through the pest coupling points concept, Roll et al. [17] developed a disease model extension coupled with the CERES-Wheat model to simulate the septoria tritici blotch impact on leaf area and yield. Pavan and Fernandes [47] conducted a study to develop a generic disease model that can be parameterized to simulate the disease cycle of several crop diseases. This model was dynamically linked to CSM through the PEST subroutines inside the CROPGRO-Soybean crop module to estimate the effects of a fungal disease on soybean [48].

The recent efforts for simulating pests and disease in wheat crops were broadly focused on wheat pathogens that reduce leaf area and photosynthesis. However, this project offers a generic approach for simulating pest damage on any plant part of wheat and a multiple disease modeling approach for simulating fungal disease effects on yield through the Generic Disease model [47].

2.4 GENERIC DISEASES MODULE

Pavan and Fernandes [47] developed a generic disease model. The model can be parameterized to simulate multiple diseases that occur in a given crop. The generic disease model was structured following the principles for coupling host and disease dynamics introduced by Berger and Jones [49]. The disease dynamics were handled at the cohort level [50]. The model was designed to represent in details the disease progress and mimic the disease life cycle. When simulating leaf spotting disease, for example, each leaf is regarded to an individual cohort of new leaf tissue resulted from the simulated growth and it is assumed as a potential infection site. The disease onset is resulted of airborne initial inoculum locally or externally produced. Under favorable environmental conditions infection takes place forming an invisible lesion. At the end of latent period, the lesion becomes visible or infectious and enlarge with time. At the infectious stage, a proportion of spores produced are distributed at three scales of spatial hierarchy [51]. The rate of infection of a potential site is computed according to ratios of autodeposition, allo-leaf-deposition and allo-plant-

deposition. The model then estimates the total diseased area based on leaf area bearing lesions and leaf area infected but with non-visible symptoms. The daily leaf area estimated by the model is reduced according to the diseased area calculated by the generic model. This approach directly affects plant photosynthesis and, consequently, the growth and final grain yield. On this study, the Generic Disease Model was parameterized to simulate the disease cycles of three major wheat diseases: powdery mildew (*Blumeria graminis f. sp. tritici*), tan spot (*Pyrenophora tritici-repentis*), and fusarium head blight (*Gibberella zeae*).

3. COUPLING PESTS AND DISEASES WITH A WHEAT CROP SIMULATION MODEL

3.1 ABSTRACT

Wheat is one of the most important global staple crops and is affected by many different pests and diseases. Depending on the pest and disease intensity, these can cause significant economic losses and even crop failure. Pest models can assist in decision-making and help reduce crop losses. Most of the current wheat simulation models account for abiotic stresses such as drought and nutrients, but they do not account for biotic stresses caused by pests and disease. The objective of this study was to couple a pest module to the Cropping System Model (CSM)-NWheat model. Coupling points were integrated into the CSM-NWheat model for applying daily damage to all plant components, including leaves, stems, roots, and grains; the whole plant, and to the assimilate supply. The coupled model was tested by simulating a wheat crop with virtual damage levels applied at each coupling point. Measured foliar damage caused by tan spot (Pyrenophora tritici-repentis) was also simulated. Compared with the observed data, the modified model accurately estimated the reduction in leaf area growth and yield loss. With the incorporation of the pest module into the the CSM-NWheat model, it can now predict the potential impact of insect pests and diseases on wheat growth and development and ultimately yield.

3.2 INTRODUCTION

Wheat (*Triticum aestivum* L.) is one of the most important cereals in the world, produced both as a human food and as a feed for livestock. Demand for wheat is expected to increase with the rise in the global population [28]. Modern wheat cultivars developed by private and public wheat breeding programs often exhibit extensive geographical adaptation [1]. Depending on the mega-environment, wheat yield and quality are constantly at risk due to numerous insect pests and diseases [52, 53]. The rapid evolution of wheat agrosystems in recent decades has led to a large variation and variability of crop losses from insect pests and plant pathogens [54, 55]). They are estimated to be responsible for 10.1 to 28.1% of global production losses [2].

With computational advancements during the past 30 years, decision support systems have been used in agriculture to help evaluate appropriate farm management technologies and to assist with complex decision-making [56, 34, 14, 57]. These agricultural risk assessment tools incorporate growth models that simulate crop development and yield through mathematical equations as a function of weather conditions, soil characteristics,

and crop management. The Decision Support System for Agrotechnology Transfer (DSSAT) computes the soil-plant-atmosphere dynamics to predict crop development and can help decision makers with selecting optimal management responses [36, 14]. The main modeling engine of DSSAT, the Cropping System Model (CSM), simulates yield for more than 42 crops and has three different modules for simulating wheat growth and development: CROPSIM-Wheat [18], CERES-Wheat [58], and NWheat, the newest wheat crop growth module incorporated in CSM [19].

Crop growth simulators have the potential to quantify and predict the effects of pests and pathogens in crop growth [57, 59, 60]. However, the risk assessments of plant pests and pathogens are usually ignored in crop simulation models [5]. In the early 1980s, attempts to evaluate pest impact on crop growth started when [61] developed Soybean Integrated Crop Management (SICM) coupled to a soybean crop model called SOYGRO [8]. This coupled system simulates the velvet-bean caterpillar population dynamics and pest-management strategies. At the same time, Boote et al. [10] classified and categorized the impact of insect pests and diseases on the type of damage they cause in plants. Boote et al. [10] identified seven pest damage mechanisms: a stand reducer, a photosynthetic rate reducer, a leaf senescence accelerator, a light stealer, an assimilate sapper, a tissue eater or consumer, and a turgor reducer, as a general method to incorporate the impact of pests and diseases into crop models. Jones et al. [11] extended the SICM pest damage modeling capabilities by estimating the effects of corn earworm (Heliothis zea) and southern green stink bug (Nezara viridula) on soybean.

In the early 1990s, Batchelor et al. [12] developed a general framework for applying pest damage coupled with the SOYGRO and PNUTGRO, a peanut crop model [62] through pest linkages, called coupling points, associated with rate and state variables for which pest damage can be expressed. This framework uses field pest-scouting data to interpolate damage between scouting dates, thus predicting crop losses due to pests and pathogens. Pinnschmidt et al. [13] estimated pest and disease effects on rice crops using the CERES-Rice module and a similar pest framework, although it was never included in the official CSM source code. These attempts to couple crop models with pests and diseases would later become a generic pest framework named PEST as part of the CSM model of DSSAT [41]. In a recent effort, Magarey et al. [16] created a simple generic infection model to predict infection periods of fungal foliar pathogens based on weather conditions. Pavan and Fernandes [47] developed a generic disease model that can be parameterized to simulate the disease cycle of several crop diseases. This model was dynamically linked to CSM through the PEST subroutines inside the CROPGRO-Soybean crop module to estimate the effects of a fungal disease on soybean [48]. Batchelor et al. [63] simulated the impact of leaf necrosis on maize yield due to lethal maize necrosis (MLN) using the PEST module coupled with CERES-Maize, a maize crop growth module of CSM.

Although the current advances in coupling crop and pest modules, most dynamic wheat simulation models still do not account for pests and diseases' damage. Willocquet et al. [15] developed a model named WHEATPEST for estimating the effects of specific pests and diseases on wheat yield. This model uses mean temperature and solar radiation, and an array of driving functions and parameters to simulate production and daily injuries caused by the pest to simulate the effects on yield loss. Whish et al. [4] estimated the impact of wheat rust on the green leaf area of wheat crops by coupling the Agricultural Production Systems Simulator (APSIM) with a rust model developed in the DYMEX population-modeling platform. Common wheat diseases such as rusts, blotches, and scab [64], currently contribute to yield losses, yet, wheat crop modules have not been dynamically coupled with a generic pest and disease framework. Understanding the biotic impact of pests and disease on wheat yield and development would be a fundamental step towards predictive agriculture and would provide useful predictions for real-farm conditions [5]. The objectives of this study were, therefore, to implement, the pest and disease coupling points in a dynamic wheat module and couple it to the PEST generic framework; to conduct a sensitivity analysis of the dynamic coupled model to evaluate its response to virtual damage levels applied for each coupling point; to evaluate its performance for a real-world case study.

3.3 MATERIALS AND METHODS

3.3.1 Applying pest and disease damage in crop modules

The estimation of the impact of pests and pathogens in CSM requires communication between a crop module and another module that handles disease damage, here referred to as the PEST module. The communication links are named as coupling points and can reduce the daily state and rate variables, such as leaf, stem, root, seed growth, and several others, according to the source type of potential damage [10].

In CSM, pest damage can be applied using several methods [12, 10, 65]. Two damage methods were selected to simulate the effects of pests on wheat:

1- Absolute damage (daily rate as amount/day) - exact damage based on the recorded pest population and the pest feeding rate.

2- Observed damage (daily rate as %/day) – removal of a certain amount of mass or area as a percentage.

The coupling points were implemented in the CSM-NWheat model, using both the absolute and observed damage rate methods. The incorporated coupling points can apply daily damage for the simulated leaf area index (LAI), leaf mass, stem mass, root mass, seed mass, necrotic LAI, assimilates, and the whole/complete plant (Table 2). Changes in LAI, leaf, stem, root, seed mass, assimilate, and the whole plant are the coupling points based

on the CERES-Maize model [41] to affect the respective CSM-NWheat state variables. The necrotic LAI was implemented based on the CROPGRO model [37].

Table 2. Coupling points incorporated in the CSM-NWheat module.

Pest ID[a]	Coupling Point Name	PCPID[b]	Damage Type[c]	Module Damage Variable[d]	The State Variable in the Module that the Variable[e] Damage is Applied to
ALAD	Leaf area index, $m^2m^{-2}day^{-1}$	LAD	1	LAIDOT, $m^2m^{-2}day^{-1}$	LAI, m^2m^{-2}
PLAD	Leaf area index, $\%day^{-1}$		2		PL_LA, mm^2plant^{-1}
ALMD	Leaf mass, $gm^{-2}day^{-1}$	LMD	1	WLIDOT, $gm^{-2}day^{-1}$	PL_NIT (leaf_part), $g[N]m^{-2}$
PLMD	Leaf mass, $\%day^{-1}$		2		PLANTWT (leaf_part), $gplant^{-1}$
ASMD	Stem mass, $gm^{-2}day^{-1}$	SMD	1	WSIDOT, $gm^{-2}day^{-1}$	PL_NIT (stem_part), $g[N]m^{-2}$
PSMD	Stem mass, $\%day^{-1}$		2		PLANTWT (stem_part), $gplant^{-1}$
ARTD	Root mass, $gm^{-2}day^{-1}$	RMD	1	WRIDOT, $gm^{-2}day^{-1}$	PL_NIT (root_part), $g[N]m^{-2}$
PRTD	Root mass, $\%day^{-1}$		2		PLANTWT (root_part), $gplant^{-1}$
ASDD	Seed mass, $gm^{-2}day^{-1}$	SDM	1	SWIDOT, $gm^{-2}day^{-1}$	PL_NIT (grain_part), $g[N]m^{-2}$
PSDD	Seed mass, $\%day^{-1}$		2		PLANTWT (grain_part), $gplant^{-1}$ GPP, $No.plant^{-1}$
PNLA	Necrotic leaf area index, $\%day^{-1}$	PDLA	2	DISLA, $cm^2m^{-2}day^{-1}$	AREAH, cm^2m^{-2}
PASM	Assimilate, $\%day^{-1}$	ASM	2	ASMDOT, $gplant^{-1}$	PCARBO, $gplant^{-1}$
PWPD	Whole plant, $\%day^{-1}$	PPLD	2	PPLTD, $\%m^{-2}day^{-1}$	PLTPOP, $plantsm^{-2}$

[a]Pest Identification codes for: actual leaf area destroyed (ALAD), percentage of leaf area destroyed (PLAD), actual leaf mass destroyed (ALMD), percentage of leaf mass destroyed (PLMD), actual stem mass destroyed (ASMD), percentage of stem mass destroyed (PSMD), actual root mass destroyed (ARTD), percentage of root mass destroyed (PRTD), actual seed mass destroyed (ASDD), percentage of seed mass destroyed (PSDD), percentage of necrotic leaf area (PNLA), percentage of assimilate reduction (PASM), percentage of plants destroyed (PWPD).
[b]Coupling point identification codes for: leaf area destroyed (LAD), leaf mass destroyed (LMD), stem mass destroyed (SMD), root mass destroyed (RMD), seed mass destroyed (SDM), plant diseased leaf area (PDLA), reduction in photosynthesis (ASM), plants destroyed (PPLTD).
[c]Damage methods for daily absolute damage rate (1), daily percent damage (2).
[d]Damage variables for applying daily LAI (LAIDOT), leaf mass damage (WLIDOT), (WSIDOT), root mass damage, (WRIDOT), stem mass damage (SWIDOT), diseased leaf area damage (DISLA), assimilative damage (ASMDOT), plant population damage (PPLTD).
[e]Model state variables that are affected on a daily basis by pest damage variables: Leaf Area Index (LAI) plant leaf area (PL_LA), nitrogen in leaf (PL_NIT(leaf_part)), leaf weight (PLANT_WT(leaf_part)), nitrogen in stem (PL_NIT(stem_part)), stem weight (PLANT_WT(stem_part)), nitrogen in seed (PL_NIT(seed_part)), seed weight (PLANT_WT(seed_part)), grain number (GPP), healthy leaf area index (AREAH), potential dry matter production (PCARBO), plant population (PLTPOP).

The pest coefficient file (FileP) defines the coupling points with the crop module for each individual pest and disease and the associated damage pattern [12]. The actual observed pest or disease incidence observed through scouting reports can be defined in the time series data file (FileT), which is read and converted into daily damage using linear interpolation. This file also contains observed data for comparison with the simulation results [41]. Alternatively, dynamic information about the actual pest or disease population or incidence can be provided through linkage of the crop model with a dynamic pest model or incorporation of dynamic pest modules into the crop model [48].

When pest or pathogens causes damage to a specific plant part weight, the state variable corresponding to the daily weight of that plant part is reduced by:

$$P(x)_t = P(x)_t^* - (\frac{Dam_t}{Pop_t}) \tag{1}$$

Where $P(x)_t$ is the state variable of a specific plant part x on day t, after damage has been applied, $P(x)_t^*$ is the state variable of a specific plant part x on day t, before applying pest damage, Dam_t is the total amount of damage applied to the state variable on day t and Pop_t is the plant population on day t.

The nitrogen available for the specific plant part is reduced according to the damage applied:

$$N(x)_t = N(x)_t^* - (\frac{N(x)_t^* \times (Dam_t \div Pop_t)}{P(x)_t}) \tag{2}$$

Where $N(x)_t$ is the nitrogen available on a specific plant part x on day t, after damage has been applied and $N(x)_t^*$ is the nitrogen available for a specific plant component x on day t, before applying pest damage.

The coupling points for leaf mass, stem mass, root mass and seed mass use these equations to apply pest damage to a respective plant part with the corresponding damage variable. The coupling point for LAI computes the daily leaf area damage (LAIDOT) caused by pests, which is subtracted from the daily LAI state variable (LAI) by:

$$LAI_t = LAI_t^* - (\frac{LAIDOT}{10000}) \tag{3}$$

Where LAI_t is the LAI (m^2m^{-2}) on day t, after damage has been applied, LAI_t^* is the LAI (m^2m^{-2}) on day t, before applying pest damage, and $LAIDOT$ is the leaf area consumed by pests ($cm^2m^{-2}day^{-1}$).

When a pest causes damage to the wheat grains, in addition to reducing grain weight, the grain number per plant (GPP) is adjusted in proportion to the seed mass loss:

$$GPP_t = GPP_t^* - (\frac{SWIDOT \div PLTPOP}{SDWT_t}) \tag{4}$$

Where GPP_t is the grain number ($no.plant^{-1}$) on day t, after damage has been applied, GPP_t^* is the grain number (no. plant^{-1}) on day t, before applying pest damage, $SWIDOT$ is the seed loss due to pests ($gm^{-2}day^{-1}$), $PLTPOP$ is the plant population ($plantsm^{-2}$) and $SDWT_t$ is the seed weight on day t, after damage has been applied, ($gplant^{-1}$).

Plant necrosis due to diseases affects the canopy photosynthesis potential on day t by reducing the healthy LAI:

$$AREAH_t = (LAI_t^* \times 10000) - DISLA \tag{5}$$

Where $AREAH_t$ is the area of healthy leaves (cm^2m^{-2}) on day t, after damage has been applied, and $DISLA$ is diseased leaf area ($cm^2m^{-2}day^{-1}$).

Sap-sucking pests cause a reduction in plant development by removing soluble assimilates from the host cells [10]. The simulation of these pests in CSM-NWheat is done by reducing the potential daily dry matter production:

$$PCARBO_t = PCARBO_t^* - ASMDOT \tag{6}$$

Where $PCARBO_t$ is the potential dry matter production ($gplant^{-1}day^{-1}$) on day t, after damage has been applied, $PCARBO_t^*$ is the potential dry matter production ($gplant^{-1}day^{-1}$) on day t, before damage was applied and $ASMDOT$ is the reduction in photosynthesis due to pests ($gm^{-2}day^{-1}$).

If pest or disease damage compromises the overall plant structure, the plant number is reduced according to the percentage of plants destroyed on day t (PPLTD):

$$PLTPOP_t = PLTPOP_t^* - (\frac{PLTPOP_t^* \times PPLTD}{100}) \quad (7)$$

Where $PLTPOP_t$ is the plant population ($plants m^{-2}$) on day t, after damage has been applied, $PLTPOP_t^*$ is the plant population ($plants m^{-2}$) on day t, before applying pest damage and PPLTD is the percent of plants destroyed, $\%m^{-2}day^{-1}$).

The LAI state variable is adjusted in proportion to the amount of plants destroyed:

$$LAI_t = LAI_t^* - (\frac{PLTPOP_t}{100}) \quad (8)$$

3.3.2 Simulating the impact of pests on wheat yield

The time series file (FileT) of a wheat experiment conducted in Kansas, USA in 1981 and included in DSSAT (KSAS8101.WHX, treatment 2 - Dryland; 60 kg N ha^{-1}) was adapted to serve as a proof of concept and to study the capability of the newly incorporated coupling points to simulate the impact of wheat diseases and insect pests. Hypothetical damage was applied for each coupling point according to the specific pest or disease of various studies (Table 3) to simulate the impact of leaf defoliation on yield loss.

Table 3. Observed pest and disease damage recorded in various studies. The damage rates (%) reported in these studies were used to evaluate the functionality of the coupling points for wheat.

Coupling Point	Pest/Disease	Damage Rate	Reference
Leaf area index	Corn Earworm (Heliothis zea)	12% - 25%[d]	Batchelor et al. (1989)
Leaf mass	Cotton Bollworm (Helicoverpa armigera)	18.5% - 28% [y]	Rogers et al. (2010)
Stem mass	Stem Rust (Puccinia graminis)	10% - 45% [y]	Loughman et al. (2005)
Root mass	Nematodes (Pratylenchus thornei)	12% - 15% [y]	May et al. (2016)
Seed mass	Fusarium head blight (Fusarium Graminearum)	18.6% [y]	Reis and Carmona (2013)
Necrotic leaf area index	Tan Spot (Pyrenophora tritici-repentis)	9% - 29% [y]	Bhathal et al. (2003)
Assimilate	Aphids (Sitobion avenae)	16% [y]	Rabbinge et al. (1984)

[d] Defoliation
[y] Yield

3.3.3 Study case

An on-farm experiment was conducted in 2016 in an area of approximately one ha in the middle of a commercial-sized agricultural field in Carazinho, Rio Grande do Sul - Brazil (28 °13'46 "S, 52 °54'32" W and 517 m). The farm had adopted a soybean–wheat crop rotation under no-tillage. Tan spot [28], a fungal disease caused by Pyrenophora tritici-repentis, occurred naturally in this field. The experimental design was a randomized complete block design with four replications. The experimental plots were sufficiently large (20 m x100 m) to accommodate regular farm machinery. Seeds were planted on June 13 at a row spacing of 17 cm, and the final plant population was 376 plants m^{-2}. The treatments were disease control with fungicide and no disease control. Opera, a fungicide with protective and systemic properties, was used for controlling tan spot. The fungicide rate was 1.5 l ha^{-1} sprayed at the tillering, booting, and anthesis phenological stages. The spring wheat cultivar was BRS Parrudo [32]. Fertilizer was applied based on recommendations from soil analysis. Approximately 40 days after planting, urea was broadcast at a rate of 80 kg N ha^{-1}.

Starting on August 2, 2016, ten plants from each plot were collected at seven-day intervals. The plants were cut close to the ground and packed in plastic bags and transported to the laboratory. Upon arrival, the leaves were separated from the stem and fixed on an A4 white paper background, with transparent tape. Images from the leaves were obtained with a CCD photographic scanner.

An artificial neural network was developed using supervised classification through the the Waikato Environment for Knowledge Analysis (WEKA) [66] to classify and measure the damage caused by tan spot in wheat leaves. The algorithm was interactively trained to classify pixels in three classes: healthy, necrosis, and background. From binary images, the obtained values were: image area (I), background area (BK), necrosis area (N), and healthy area (H). The leaf area (L) was calculated by subtracting the background area (BK) from the image area (I). Then, the proportion of necrosis (K) was obtained by K = N/L.

Environmental variables were monitored using a micrometeorological tower installed in the center of the experimental area. Sensors attached to the tower measured relative humidity (%), temperature (^{o}C), global incident solar radiation (MJ m^{-2} day^{-1}), and rainfall (mm). All sensors were connected to a datalogger with channel multiplexers, and readings were taken every 30 seconds, with averages and totals stored every 15 minutes for the duration of the wheat growing season.

3.4 RESULTS AND DISCUSSION

3.4.1 Coupling points response to hypothetical damage

Hypothetical pest damage was applied to experiment KSAS8101.WHX, treatment 2, a wheat experiment included in the DSSAT library, to primarily identify the reliability and functionality of the coupling points in CSM-NWheat. In this simulation, the attainable yield at 248 days after planting with no disease damage was 3,688 kg ha^{-1}, leaf weight 1,348 kg ha^{-1}, stem weight 2317 kg ha^{-1}, root weight 1,596 kg ha^{-1}, total canopy weight 8,979 kg ha^{-1}, maximum LAI 2.7 m^2 m^{-2} and grain number 12,413 no. m^{-2}. The damage levels were applied based on Table 2 and expressed as part of the time series data file (FileT).

When damage equivalent to 25% defoliation was imposed on the LAI state variable and interpolated during mid-late season, between 169 and 214 days after planting, final yield decreased to 3,027 kg ha^{-1} (-17.9%), and leaf weight decreased to 1,018 kg ha^{-1} (-24.5%). For leaf mass, damage equivalent to 20% defoliation during the mid-season between 149-178 days after planting, resulted in a yield of 2,910 kg ha^{-1} (-21.1%) and a leaf mass of 889 kg ha^{-1} (-34.0%). Damage equivalent to a 17% of stem mass loss during the late season between 193 and 227 days after planting, resulted in a grain yield of 3,129 kg ha^{-1} (-15.1%) and a stem mass of 934 kg ha^{-1} (-59.6%). Damage equivalent to a 15% loss in the roots during the early-mid season between 56 and 167 days after planting, resulted in a grain yield of 3,177 kg ha^{-1} (-13.9%) and a root mass of 1,217 kg ha^{-1} (-23.7%) (Figure 4).

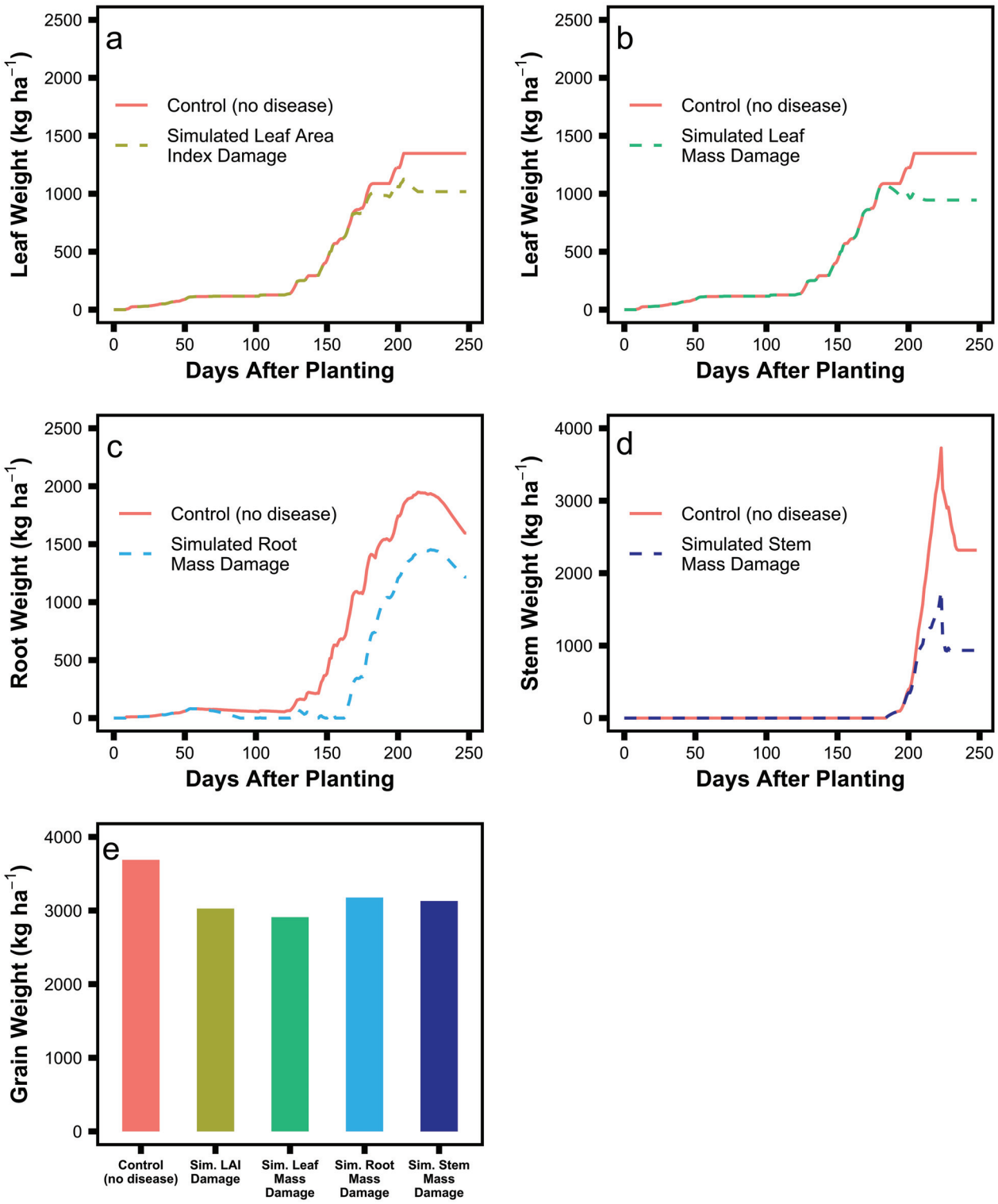

Figure 4. Response of the coupled NWheat and PEST modules to pest and disease impact as presented in Table 2 in comparison to the attainable simulations. Simulated leaf weight with hypothetical damage applied to LAI (a) and leaf mass (b); simulated root weight with hypothetical damage applied to root mass (c); simulated stem weight with hypothetical damage applied to stem mass (d); Simulated yield response to the individual instances of hypothetical damage applied to the LAI, leaf mass, root mass and stem mass state variables (e).

Leaf area necrosis virtual damage equivalent to 20% of pest necrosis was applied late during the season between 192 and 247 days after planting, resulting in a grain yield of

3,040 kg ha-1 (-17.6%), and a canopy weight of 8,249 kg ha^{-1} (-8.1%). Assimilate damage equivalent to a 17% assimilate supply loss late during the season between 203 and 241 days after planting, resulted in a grain yield of 3,093 kg ha^{-1} (-16.1%) and a canopy weight of 8,079 (-10.0%). Hypothetical damage equivalent to a 18% seed mass loss during the late season between 225 and 243 days after planting, resulted in a grain yield of 2,959 kg ha^{-1} (-19.8%) and a total number of grains of 9,192 no. m^{-2} (-26.0%) (Figure 5).

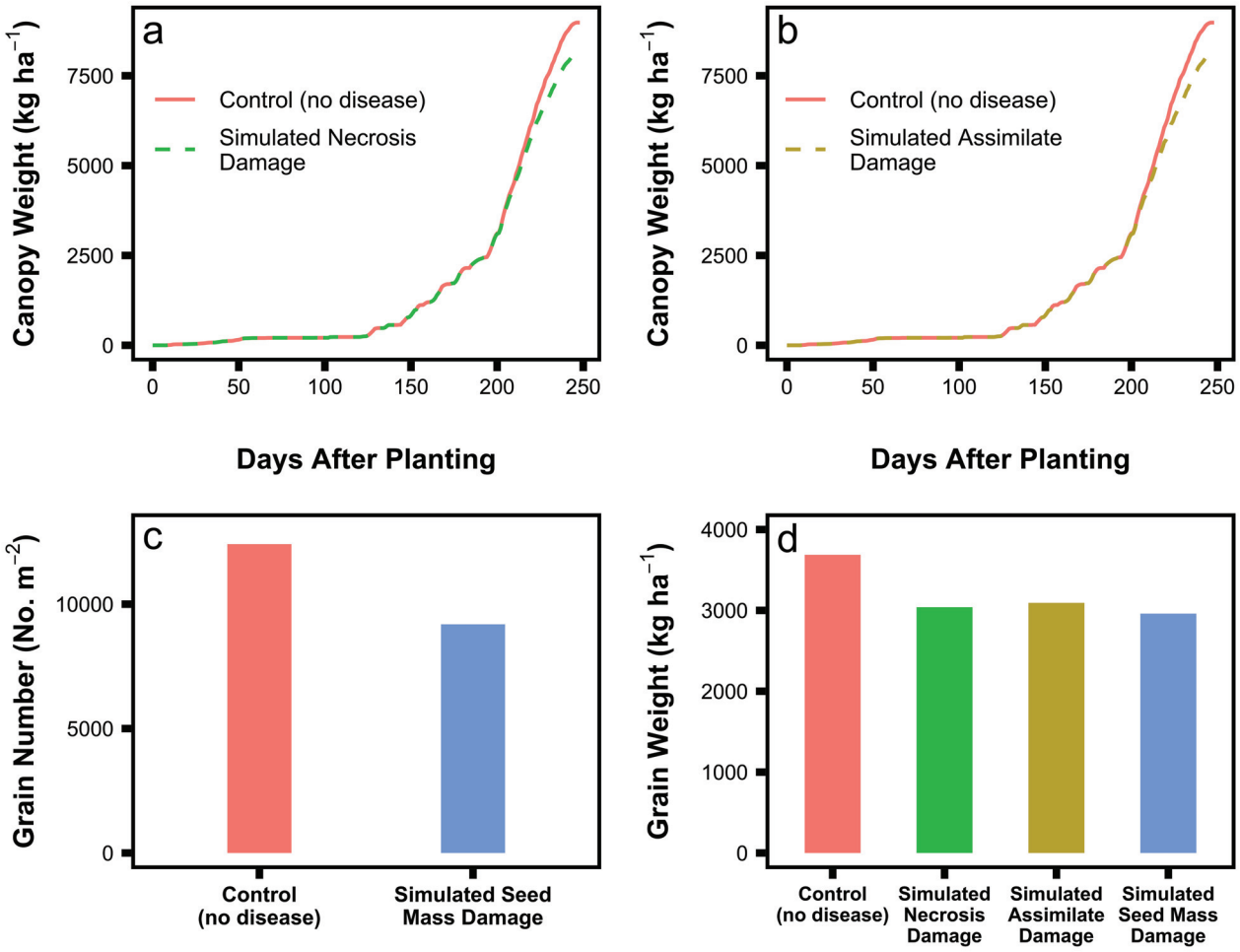

Figure 5. Response of coupled NWheat and PEST modules to pest and disease impact as presented in Table 2. Simulated canopy weight with hypothetical necrosis damage applied to LAI (a); Simulated canopy weight with hypothetical damage applied to the crop assimilate supplies (b); Simulated grain number with hypothetical damage applied to seed mass (c); Simulated yield response to the individual instances of hypothetical damage applied to the assimilate supplies, leaf area due to necrosis and seed mass state variable (d).

The model's response when individual plants are removed due to pests and pathogens was analyzed by applying hypothetical damage levels that reduced the plant population. Damage equivalent to 5%, 8%, and 10% of plants destroyed were applied as daily rate damage using the time series data file (FileT) during the mid-growing season between 169 and 191 days after planting. A 5% reduction in the plant population resulted in a yield loss of 1,088 kg ha^{-1} (-29.5%) and a maximum LAI of 2.2 m^{2}m^{-2} (-18.5%). An 8% reduction in the

plant population resulted in a yield loss of 1,668 kg ha^{-1} (-45.2%) and a maximum LAI of 2.2 m^{2}m^{-2} (-18.5%). Lastly, a 10% reduction in the plant population resulted in a yield loss of 1,994 kg ha^{-1} (-54.1%) and a maximum LAI of 2.1 m^{2}m^{-2} (-22.2%) (Figure 6).

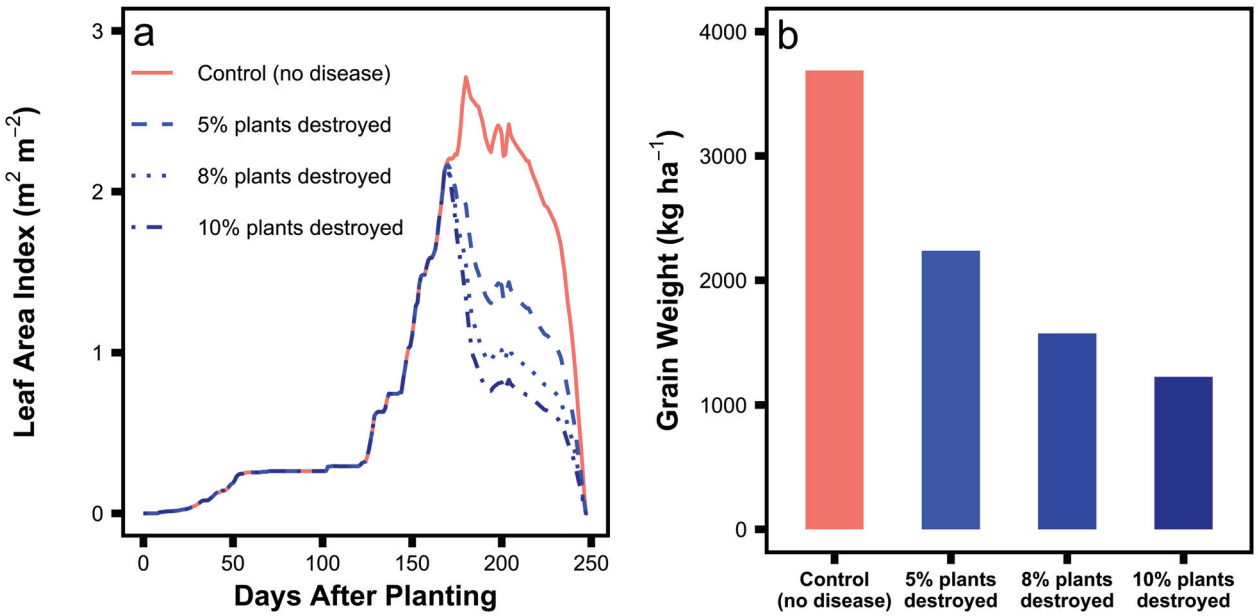

Figure 6. Sensitivity of the CSM-NWheat module coupled with the disease module to simulate the effects on LAI (a) and yield (b) when 5%, 8% and 10% of the plants are removed.

This proof of concept shows the potential of a coupled pest module with a wheat module to dynamically simulate different pest and disease infection scenarios. The coupled model was able to simulate the yield and leaf area losses due to damage caused by multiple pests and diseases on different plant components of wheat based on studies reported in the literature (Table 2). The damage levels were implemented in one of the crop model input files (FileT) following the reported chronological occurrence pattern of each pest, as reported crop losses in general depend on when a given pest or disease damage occurs. The advantage of using coupling points is that they are not bound to specific pests or diseases. Therefore, this approach can be used to simulate the impact of different insect pests and diseases on wheat growth and development as long as they have the same coupling points as listed in Table 1. Even cases with severe pest damage that kills the entire plant can be simulated.

3.4.2 Field experiment

Tan spot is caused by the fungus *Pyrenophora tritici-repentis* and is also known as yellow leaf spot or yellow leaf blotch. The ascospores or conidia of this fungus infects the host cells and induces necrosis and chlorosis symptoms on wheat leaves [28]. It starts as a small tan spot, destroying the living tissue and developing into lesions with a brown spot in the center and yellow borders [32]. Temperature and free moisture on the leaf surface are

critical environmental factors for tan spot infection [67]. This pathogen reduces the photosynthetic area of leaves, which results in substantial losses in both yield and grain quality, including reduced grain fill, a smaller number of kernels per head, and kernel shriveling [68]. Natural infection of tan spot disease occurred in the wheat field experiment that was conducted in 2016 in Carazinho, Rio Grande do Sul, Brazil. The observed yield in the control treatment with no tan spot damage was 3,915 kg ha^{-1} compared to 3,750 kg ha^{-1} in the plots where tan spot was present. On average, there was a reduction of 4.2% in grain yield due to tan spot infection. Throughout the entire experiment, the disease severity was expressed as the mean proportion of necrosis measured at each measurement date (Figure 7). These pest data of the scouting reports were entered in the time-series data file (FileT) to simulate the effect of tan spot observed on the wheat field. The damage was applied using the observed damage method (% as a daily rate) and the necrotic LAI coupling point (Table 2).

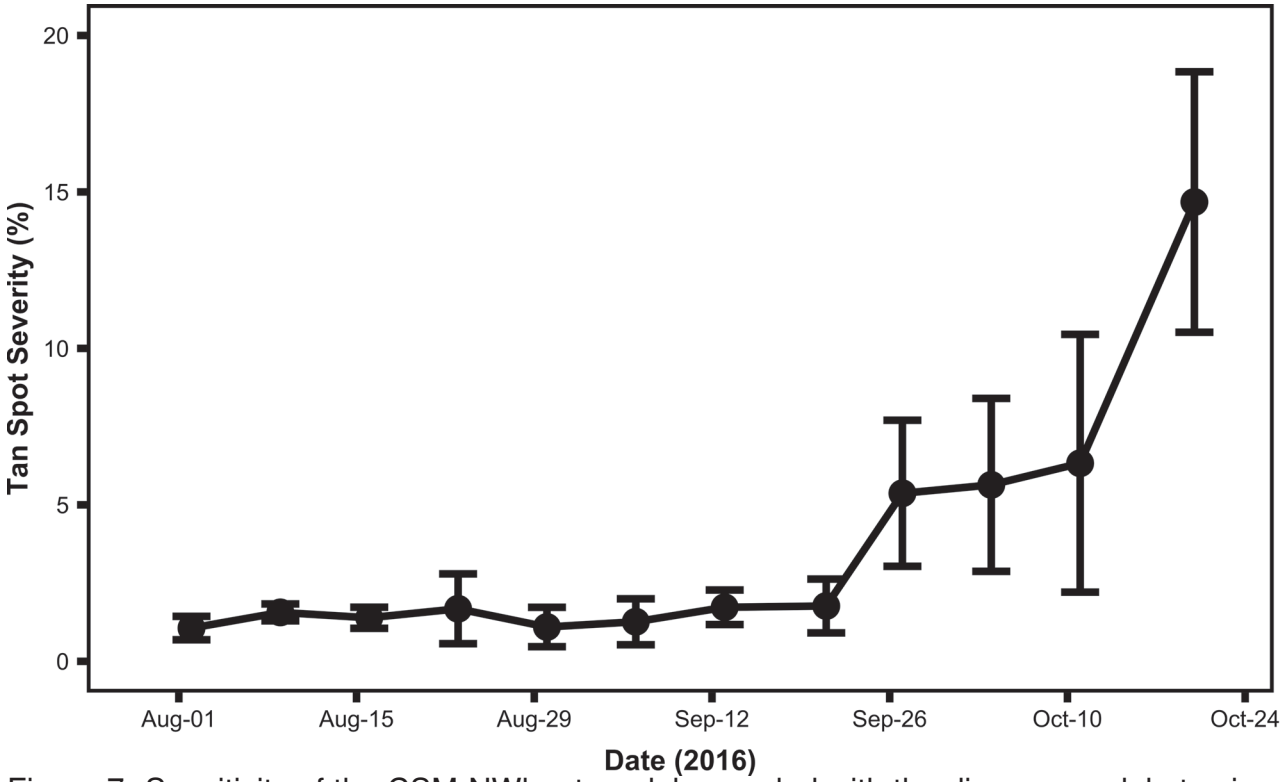

Figure 7. Sensitivity of the CSM-NWheat module coupled with the disease module to simulate the effects on LAI (a) and yield (b) when 5%, 8% and 10% of the plants are removed.

Simulated wheat yield with the new coupled NWheat and PEST modules for the treatment with no disease was 4,414 kg ha^{-1}, while the yield simulated for the treatment affected by tan spot was 4,207 kg ha^{-1} due to a reduction in leaf mass and LAI. This corresponds to a reduction in yield of 4.6% due to tan spot infection (Figure 8). Overall, the CSM-NWheat model predicted higher grain yield than the yield level that was measured in the field experiment. However, the yield loss due to tan spot infection predicted by the pest-coupled model was similar to the percentage yield loss observed in the field experiment with a slight overestimation of a 0.4% yield loss. The results of this primarily analysis indicates

that the newly coupled model is capable to simulate the potential impact of disease damage during wheat growth and development.

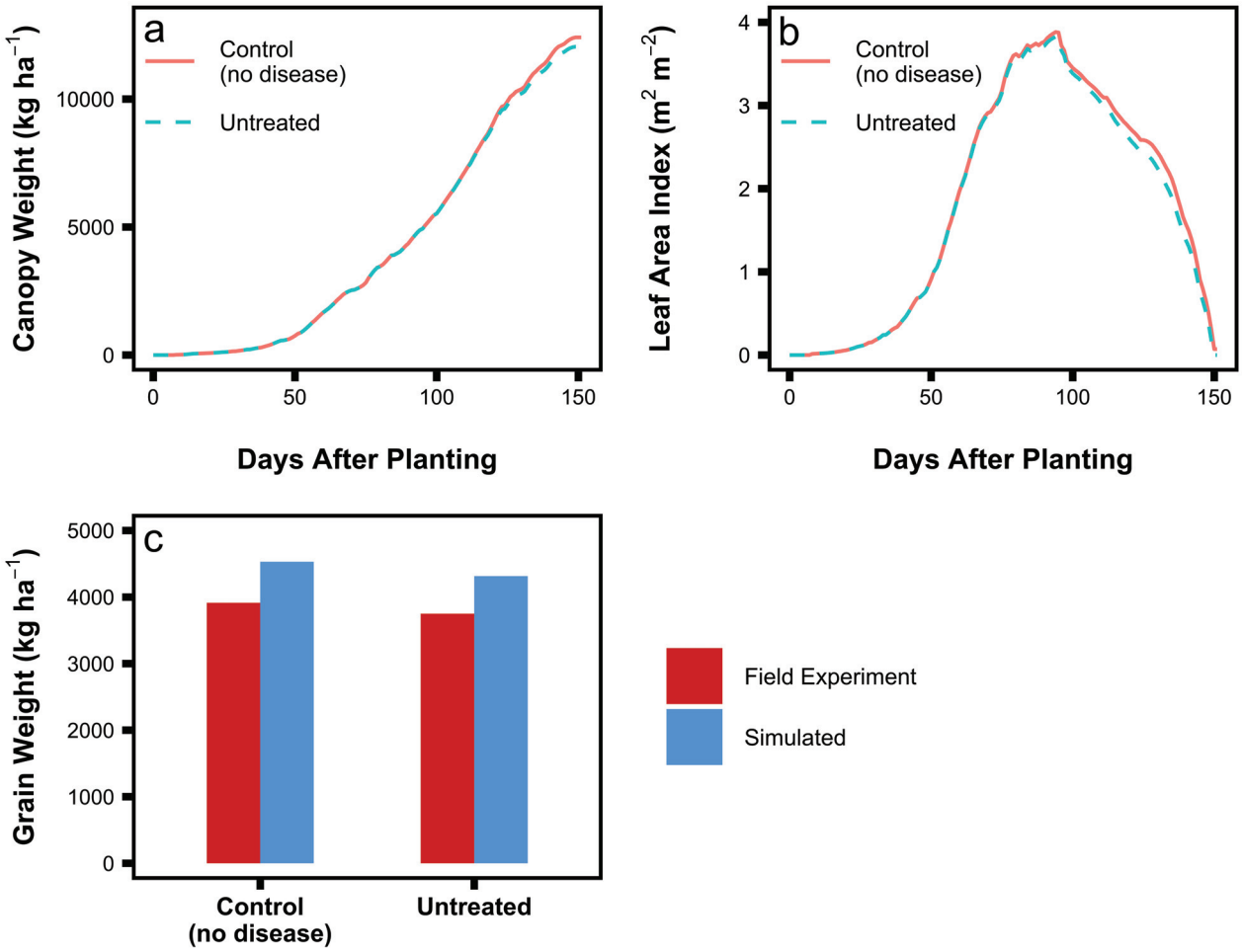

Figure 8. Natural occurring tan spot severity measured in wheat plots without fungicide applications during an on-farm experiment conducted in 2016 in Carazinho, Rio Grande do Sul, Brazil.

3.5 SUMMARY AND CONCLUSIONS

The communication links created to couple the CSM-NWheat crop growth model to the PEST module of DSSAT allow daily pest interaction with the growth and development of leaf, stem, seed, root, and the photosynthesis rate of the wheat model. The damage routines simulated wheat defoliation and yield loss according to different types of pests and diseases. A case study was used to simulate tan spot (Pyrenophora tritici-repentis) infection on wheat, and the results were compared to those observed in a field experiment. The coupling points gave the model flexibility to predict crop growth in combination with pest damage levels. Although the average leaf area loss due to tan spot infection observed in the study case was less than 5%, overall, the model had a similar response to the measured data. The

sensitivity analysis indicated the capability of the model coupled with the PEST module to predict damage similar to what was observed in the field experiments.

The newly coupled model can be applied for simulating the potential impact of insect pest and disease damage, and it is not limited to a specific pest or crop condition. This allows for the simulation of different pest scenarios for wheat following the chronological occurrence pattern of a given pest or disease and mimics the effects of pest damage on crop development and predict yield loss. Future research should include more field experimental data from a range of environments to evaluate the model's capability to estimate disease and pest effects on wheat for different management practices and environmental conditions. This research extends the functionalities of the CSM-NWheat crop model and expands its potential applications to address pest and disease-related issues occurring in real-world scenarios. This is the first wheat model in the DSSAT crop modeling ecosystem [14] that has been coupled with the pest module of DSSAT. It will allow now for the dynamic simulation of both biotic and abiotic stresses on wheat growth and development and ultimately yield.

4. ASSESSMENT OF YIELD DAMAGE CAUSED BY DISEASES IN WHEAT: A SIMULATION APPROACH USING THE NWHEAT MODEL

4.1 ABSTRACT

Simulating the damaging effects of pests and diseases on crop yield is a crucial step for predictive agriculture. In this study, we developed and evaluated an approach to simulate the damaging effects of powdery mildew (*Blumeria graminis f. sp. tritici*), tan spot (*Pyrenophora tritici-repentis*) and fusarium head blight (*Gibberella zeae*) on wheat (*Triticum aestivum* L.) yield using the CSM-NWheat model. Three independent disease models, each simulating one wheat disease, were coupled with the wheat crop model using parallel communication (MPI standards). The disease components inflict daily disease damage through specific pest coupling points if the environmental conditions are favorable for infection. The simulated powdery mildew and tan spot damage were inflicted on wheat photosynthesis rate and leaf area index. Fusarium head blight applied damage upon grain yield. This approach was tested on a two-year dataset collected in Brazil, where these fungal diseases naturally occurred throughout the experiments. The coupled model had consistent results compared with the observed data and simulated well the impact on grain yield. This multi-model approach using MPI showed the positive effect of coupling multiple specific models to accurately estimate pest and disease damage.

4.2 INTRODUCTION

The maximum yield of plants, determined by their genetic potential, is seldom achieved because factors such as inadequate water or nutrients, adverse climatic conditions, insect and disease damage will limit growth at some stage. Wheat (Triticum aestivum L.) is one of the world's main staple crops, which provides around 20% of daily protein and calories [69]. Wheat is generally affected by various fungal diseases that are considered harmful to the economy for their potential to damage crops and reduce income. Even with the current disease control methods, it has been estimated an actual yield loss of 13% [52].

The information needs for agricultural decision-making at all levels are increasing rapidly due to increased demands for agricultural products and increased pressures on land, water, and other natural resources. Over time science has been trying to anticipate phenomena and prevent epidemics from minimizing risk and increasing productivity. Decision support systems have been used for the last decades to help farmers and researchers in decision-making. These systems incorporate crop growth models that simulate crop growth and development through mathematical equations as a function of weather conditions, soil

characteristics, and crop management. These tools help create scenarios, identify unusual situations, and generate alerts, usually based on historical data. The Decision Support System for Agrotechnology Transfer (DSSAT) predicts crop growth by computing the soil-plant-atmosphere dynamics and assisting in the decision making [36, 14]. The Cropping System Model of DSSAT, the main engine of the system, can simulate crop growth for over forty-two crops and has three different modules for simulating wheat development: CROPSIM-Wheat [18], CERES-Wheat [58], and NWheat [19].

These models are available for the wider community and provide growth and crop production in the following levels: potential, attainable, or actual production. The models predict potential yield as a function of site-specific weather (solar radiation, temperature, CO2, and day length), but assuming no limitations from pests/diseases. Attainable production is predicted where constraints from water and fertility are simulated. Actual production is what farmers achieve and includes limiting factors in the field, such as soil fertility and pest-disease aspects. However, most crop models operate at the attainable yield level (considering water and N) and do not account for pest and disease effects, either mechanistically or via post-model. Failure to account for the impact of insect pests and diseases when simulating crop growth is currently one of the major limitations of most crop simulation models. In the early attempts to study crop loss due to insect pests and disease infection, Rabbinge and Rijsdijk [70] and Boote et al. [10] classified the injury mechanisms and the effects on plant morphology or physiology. Boote et al. [10] categorized the pest influence on the plant carbon flow according to the types of damage they do in the host plant.

This concept is present in the Cropping Modeling System (CSM) of DSSAT to impact crop growth and development through pest linkages named coupling points [10, 12]. These communication structures assess pests and diseases potential impacts on crop production using unique model variables whose daily-changing values represent pest and disease damage to crop organs or growth and development processes. Examples of coupling point variables include leaf mass or area, stem mass, root mass, root length, and seed mass or number, all of which might be negatively impacted by pests and diseases. Batchelor et al. [12] developed a general framework allowing the user to input field observations and scouting data on insect damage, disease severity, and physical damage to plants or plant components (e.g., grains or leaves). This module simulates the likely effects of those pests and diseases on crop growth and economic yield using linear interpolation between scouting reports to estimate the daily impact of a specific plant part. This framework and other attempts to couple pests and diseases with crop models [13] would become the PEST module, a generic pest framework of the DSSAT crop modeling platform [14].

Recently, the CERES-Wheat was coupled with a disease model for the simulation of Septoria tritici blotch in wheat [17]. CSM-CERES-Beet model had coupling points added to estimate the Cercospora leaf spot disease effects on sugar beet yield [71]. Ferreira et al. [72] also implemented pest and disease coupling points within the CSM-NWheat, a wheat

crop model, to estimate pest and disease effects on crop growth using the DSSAT's PEST module. However, coupling independent modules that simulate the entire cycle of a pest or disease to crop growth models can simplify the representation of biotic stress and the impact on crop growth [5]. A well-known example of this approach was a simple generic infection model based on weather conditions developed to predict fungal plant pathogens [16]. Pavan and Fernandes [47] also demonstrated this concept with the Generic Disease Model (GDM), which can be parameterized to simulate multiple diseases in a given crop. This approach, however, has not been applied to simulate pests and disease damage on wheat. The objectives of the present study were 1) to parameterize the Generic Disease Model to mimic the fungal life cycle of *Blumeria graminis f. sp. tritici*, *Pyrenophora tritici-repentis* and *Gibberella zeae*, the causing agents of powdery mildew, tan spot, and fusarium head blight of wheat, respectively, 2) dynamically link these models to the CSM-NWheat crop model through the coupling points, and 3) to predict the impact of these fungal diseases on wheat yield.

4.3 MATERIAL AND METHODS

4.3.1 Crop and disease modeling

Recently, Ferreira et al. [72] developed a disease extension inside the CSM-NWheat for simulating pest and disease damage in wheat. The implemented pest and disease subroutines allowed the linkage between the crop model and the Generic Disease Model [47]. The model was parameterized to simulate the disease cycles of powdery mildew (PM), tan spot (TS) and fusarium head blight (FHB). Powdery mildew in wheat is a disease that affects leaves and stems, producing white powdery spots that reduce the efficiency of photosynthesis [31]. The spores infect the host cells through penetration pegs causing the plant to shunt resources to the fungus. Tan spot, also known as yellow leaf spot or yellow leaf blotch induces necrosis and chlorosis symptoms on wheat leaves [28]. The fungus destroys the living tissue expanding into lens-shaped lesions with a brown spot in the center and yellow borders [32]. Fusarium head blight, also known as gibberella or scab, infects the wheat grains and produces a mycotoxin named deoxynivalenol (DON) causing tissue necrosis inside the kernels [25]. This can lead to lightweight seeds and reduced kernel set and its contamination can have risk to human and animal health [73]. The parameters for the disease models were extracted from the literature or empirically set by wheat diseases experts. Multiple independent instances of the GDM were created to predict the individual impact of the diseases on wheat growth. Each disease component inflicts daily disease damage through damage variables if the conditions are favorable for infection.

Favorable conditions for infection for these fungi diseases are climates with moderate temperatures, high relative humidity and free moisture in the plant's surface.

Weather variables such as temperature, relative humidity, rainfall and solar radiation provided on an hourly basis governs the disease's progress. The generic disease model was structured following the principles for coupling host and disease dynamics introduced by Berger and Jones [49]. Disease dynamics were handled at the cohort level [50]. In the wheat model, each leaf/seed was regarded as an individual cohort of new tissue resulting from simulated growth and it was assumed to be a potential infection site. Disease onset resulted from airborne initial inoculum locally or externally produced. Under favorable environmental conditions, infection takes place forming an invisible lesion. At the end of the latent period, the lesion becomes visible or infectious and enlarges with time. At the infectious stage, a proportion of spores produced are distributed at three scales of spatial hierarchy [51]. The rate of infection of a potential site is computed according to ratios of autodeposition, allo-leaf-deposition and allo-plant-deposition. It was assumed that the diseased area resulted from the totalization of the leaf area bearing lesions and leaf area infected but with non-visible symptoms. The diseased area is then used to update the leaf area variable estimated by the crop model which will directly impact the plant photosynthesis, growth rate and, consequently, the final grain yield. This method was used to simulate powdery mildew and tan spot on wheat. The simulated fusarium head blight, affected the seed state variable of the model. The FHB daily spore production was computed using the GibSim [74]. This model assumes the *Gibberella zeae* inoculum is present in the surface of the soil residue and the airbourne propagules spread in the environment using a function for spore dispersion and deposition which estimates the daily density of the spore cloud. The number of spores was translated into damage according to the infection rate. The other two components assume sporulative powdery mildew and tan spot lesions are present in the environment in which prediction is made and estimates the rate of conidiophore development as a function of temperature and relative humidity.

The communication between models was established using OpenMPI, a Message Passing Interface (MPI) library for parallel computing [75, 48]. MPI was adopted as a standard method of communication due to the availability and portability of libraries for multiple languages. The Multiple Instruction, Multiple Data (MIMD) approach was used to achieve parallelism and information exchange in daily steps throughout the simulations. MIMD allows multiple independent programs to execute simultaneously sharing data among each other through an MPI interface [76]. This interface provides an easy data exchange between the disease models, written in C++, and the wheat crop growth model, written in Fortran (Figure 9).

During the simulation, the CSM-NWheat sends to the three disease models the daily values of leaf mass, seed mass and LAI state variables. Based on the weather data and specific disease parameters, the disease models estimate the daily spore production and cloud density. Whenever there are appropriate conditions for disease infection, spores present on the field and the received values of the state variables are greater than zero, the

disease models simulate in daily steps the disease life cycle and returns to the wheat model the respective damage through a specific damage variable. Lastly, the wheat model receives the data and applies the reduction on the state variables and the process is repeated for each day until the end of the simulation.

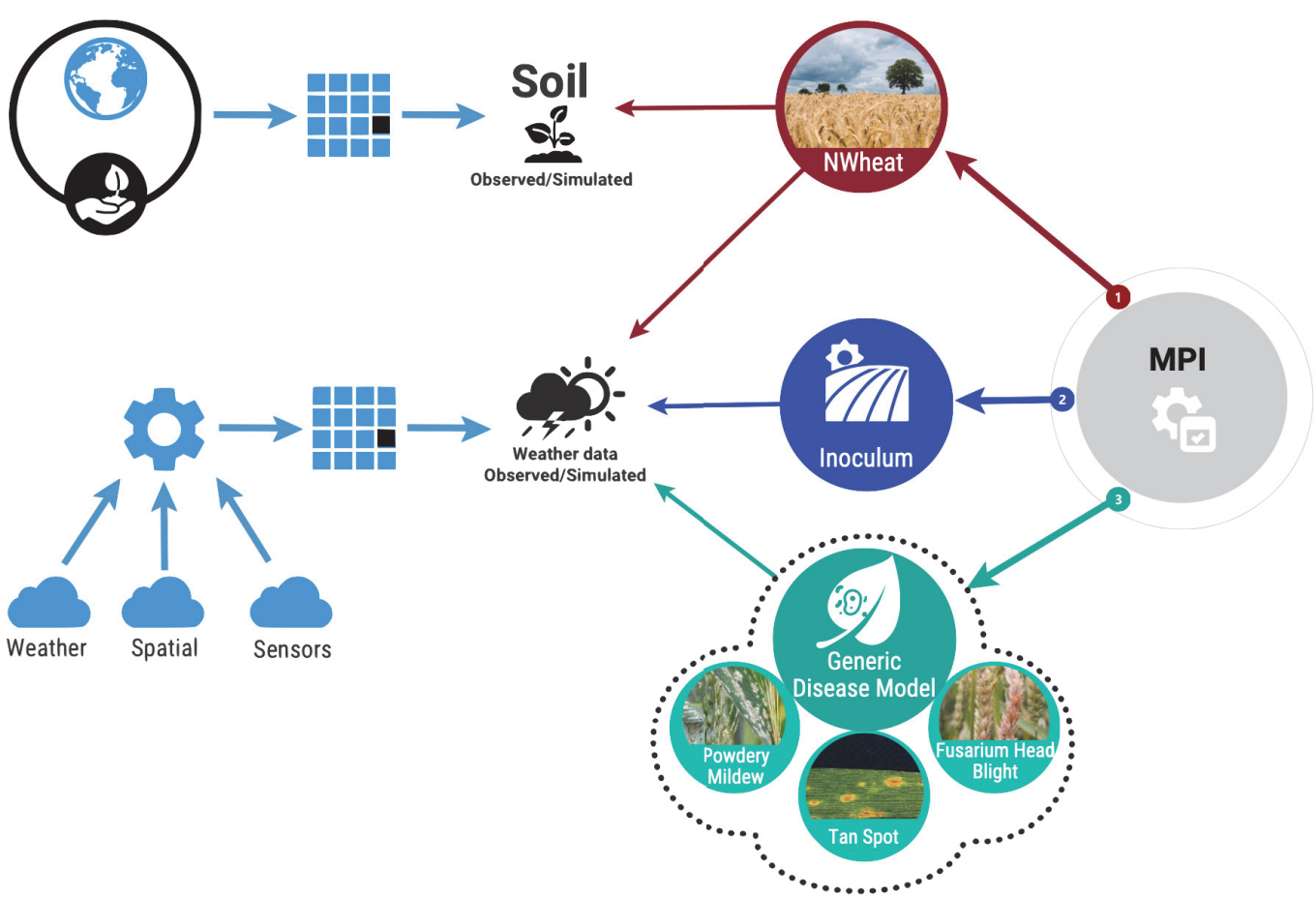

Figure 9. Diagram of system functionality and communication.(1) The communication starts with the CSM-NWheat sending to the three disease models the daily values of leaf mass, seed mass and LAI state variables. (2) The disease models, on the other hand, are computing the daily spore production and cloud density. (3) Whenever there are appropriate conditions for disease infection, spores present on the field and the received values of the state variables are greater than zero, the disease models simulate in daily steps the disease life cycle and returns to the wheat model the respective damage through a specific damage variable. Lastly, the wheat model receives the data and applies the reduction on the state variables and the process is repeated for each day until the end of the simulation.

4.3.2 Experimental data

Field experiments were carried out in 2018 and 2019 at an experimental area of Embrapa Trigo in the municipality of Coxilha, RS, Brazil. The first experiment was conducted in an area with 10% slope and east exposure (28°11'11"S, 52°19'31"W and 688m above sea level). The second experiment was carried in a flat area close to the first experiment in succession to crotalaria crops (*Crotalaria juncea L.*) and turnip (*Raphanus sativus L.*), respectively. The climate in the region is Cfa (Humid subtropical climate) according to the classification of Köppen [77]. The soil is an Aluminoferric Red Latosol [78] with the 2019 experiment soil originating from horizon B, due to the removal of the A horizon in the past. The experimental design was a randomized block design with five replications. The plots

were 6-m long and 4.42-m wide, totaling 26.52 m², in 2018 and 15-m long and 2.21-m wide, totaling 33.15 m² in 2019.

Before sowing, the areas were desiccated, with specific products for each condition. The desiccation was carried out on 06/15/2018 and 07/02/2019, aiming at eliminating the remaining invaders. The wheat cultivar TBIO Toruk used for both experiments and was sowed on July 02, 2018 and June 24, 2019. The emergence date was on July 10, 2018 and July 04, 2019 while the harvesting date was on November 13, 2018 and November 11, 2019, respectively. The line spacing adopted was 17 cm in both experiments with a density between 300-400 seeds m^{-2} in 2018 and 400-450 seeds m^{-2} in 2019. The wheat seeds used did not receive phytosanitary treatment before sowing in 2018, while in 2019 they were treated with difenoconazole, imidacloprid, and thiodicarb.

Nitrogen was broadcasted as urea at 120 N kg ha^{-1} in 2018 and 100 kg ha^{-1} in 2019 and both were divided into two applications. In the first experiment, the applications were carried out on 08/10/2018 and 09/11/2018 and in the second experiment were on 07/26/2019 and 08/28/2019. There were four treatments which three had fungicide application under different regimes and one with no disease control. In 2018, the fungicide Opera and the insecticide Premio were sprayed at a 7-day, 14-day and 21-day intervals on the disease control treatment with a rate of 0,75L ha^{-1} and 0,05L ha^{-1}, respectively. During the experiment in 2019, the fungicide Nativo (0,6L ha^{-1}) and the insecticide Premio (0,1L ha^{-1}) were applied under the same spraying regime used in the previous year. Each experiment had the fungicide and insecticide solved in 150 L water for application per hectare.

The monitoring of wheat phenology started with the emergence of plants and was carried out throughout the cycle. Weekly the phenological stages were recorded according to the phenological scales of Zadoks et al. [79]. After emergence, the plants were collected at 7-day intervals. The plants were cut close to the ground and packed in plastic bags. Upon arriving in the laboratory the leaves of each plant were separated from the stem and fixed in a white paper base, with transparent tape. Subsequently, the sheets were scanned in the LICOR scanner, 3100-L model and 0.1 mm^2 pixel resolution, and the images were used for calibration and validation of the software. The plants were also dissected to determine the dry matter mass of green leaves (LFWT), dry leaves (DLWT), stem (STWT), ears (EAWT) and grains (SDWT). The leaf area index (LAI) was determined at 15-day intervals through an optical planimeter to measure the leaf area (LA) of green leaves. The specific leaf area was determined using the leaf area and the dry matter mass of green leaves:

$$LA = a + bLFWT \tag{9}$$

where LA is the leaf area of wheat (cm^2); $LFWT$ is the dry matter mass of green leaves (g); a and b are the linear and angular coefficients of the adjusted simple regression,

respectively. In the present case, a is the coefficient and b is the specific leaf area for wheat in cm^2 g^{-1}. The weekly LAI for wheat was calculated by:

$$LAI_i = \frac{LAI_i}{A} \tag{10}$$

where LAI_i is the leaf area index on day i; LA_i is the leaf area of wheat on day i; A is the soil area occupied by the sample of $LFWT$.

Grain yield was determined when the wheat plants reached maturity. Sampling was done in the central part of the plot area, where the lines were not collected for dry matter mass estimation. In both experiments, the grains were separated and the impurities were removed by passing the sample in an electric blower, with controlled air flow. Then the moisture content of the grains of each plot was determined (AL-101, AGROLOGIC). The grain yield was corrected to 13% moisture and calculated for an area of one hectare. The hectoliter weight was determined through the samples. A fraction of samples were used to determine the thousand grains dry matter weight corrected to 13% humidity. The number of grains per m^{-2} was calculated based on the resulting dry matter weight and the grain yield of the plot.

For the monitoring of environmental variables, a micrometeorological tower was installed beside the experimental area in 2018 and about 300 m from the experiment in 2018. Attached sensors to the tower measured temperature and relative humidity (AT2/RHT2, Delta T), global incident solar radiation (ES2-05,Delta T) and rainfall (ARG100, Delta T) (Figure 10). All sensors were connected to a datalogger (CR1000, Campbell Scientific, Inc), with channel multiplexers and readings were taken every 30 seconds, with averages and/or totalization, stored every 15 minutes during the whole wheat season. Relative humidity data collected from stations in the county of Passo Fundo, Rio Grande do Sul, Brazil (28 °13'48.0" S 52° 24'36.0" W) was also incorporated to estimate the spore cloud density weeks before the sowing dates of each experiment.

Leaf-wetness sensors (LWS - Dielectric Leaf Wetness Sensor, Deacon Devices) were installed in metal rods one meter high with a sliding system according to the crop growth and/or data objective. These sensors were placed after the sowing date for both experiments at the base of the canopy level and 80 cm above ground. The sensors in the base of the plant were weekly elevated to stay at the top of the canopy until it reached 40 cm above ground and the same level was kept until harvesting date. After that, the sensors at 80 cm above ground were lowered the spike level and were weekly adjusted to continue the leaf wetness readings at the top of the canopy level. When the crop reached maturity, the sensors at the highest level were placed at the wheat ears level. Leaf wet periods were calculated by the time the sensor reading showed values equal to or greater than 284 mV, as specified in the sensor manual. The collected data from the leaf-wetness sensors was

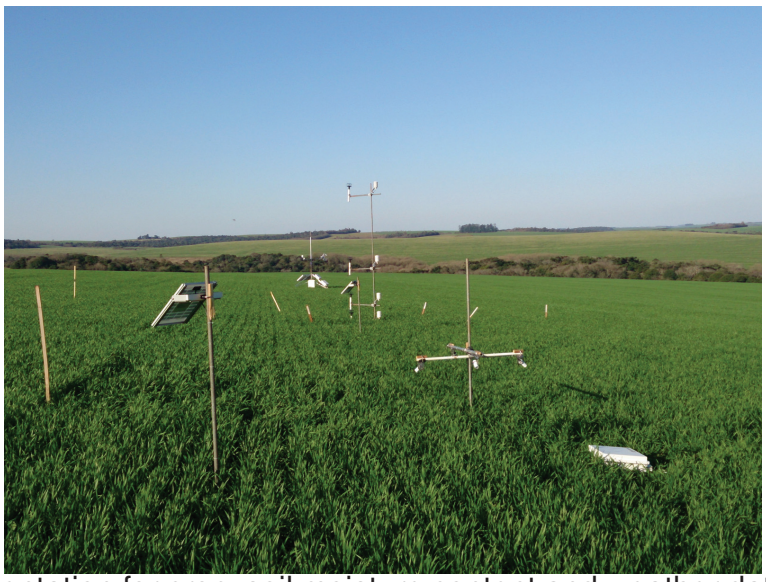

Figure 10. Instrumentation for crop, soil moisture content and weather data monitoring at an experimental area in the municipality of Coxilha, RS, Brazil.

used to identify the daily number of hours that moisture was available on the plant's surface area for spore germination.

4.3.3 Disease data acquisition

Trainable Weka Segmentation (TWS) is a Fiji [80] plugin with state-of-the-art machine learning algorithms provided by WEKA [66] a toolkit for data analysis and predictive modeling. TWS can classify pixels as belonging to a specific class determined by the user. Weka provides methods such as supervised classification, regression, and clustering to develop and build a machine learning classifier. The plugin offers an interface for interactive learning and provides feedback to the user. Once the classifier is trained, it can be applied to other images in an automatic way using features like macro programming provided by Fiji platform.

Fiji and TWS were used to classify and measure the damage caused by fungal diseases in wheat leaves. These tools allowed to compare and analyse the performance of several machine learning and image processing approaches. Images are obtained by scanning wheat leaves using a CCD photographic scanner. All images have a uniform background. Initially, a classifier was interactively trained to classify pixels in three classes: healthy, necrosis, and background. This step comprises selecting the areas using the tools provided by Fiji in a sample image and assigning them to one of the three classes available (Figure 4). This step requires specialist knowledge to ensure classification process efficacy. Once classifier training is finished, the developed model can be applied for classifying field collected leaves.

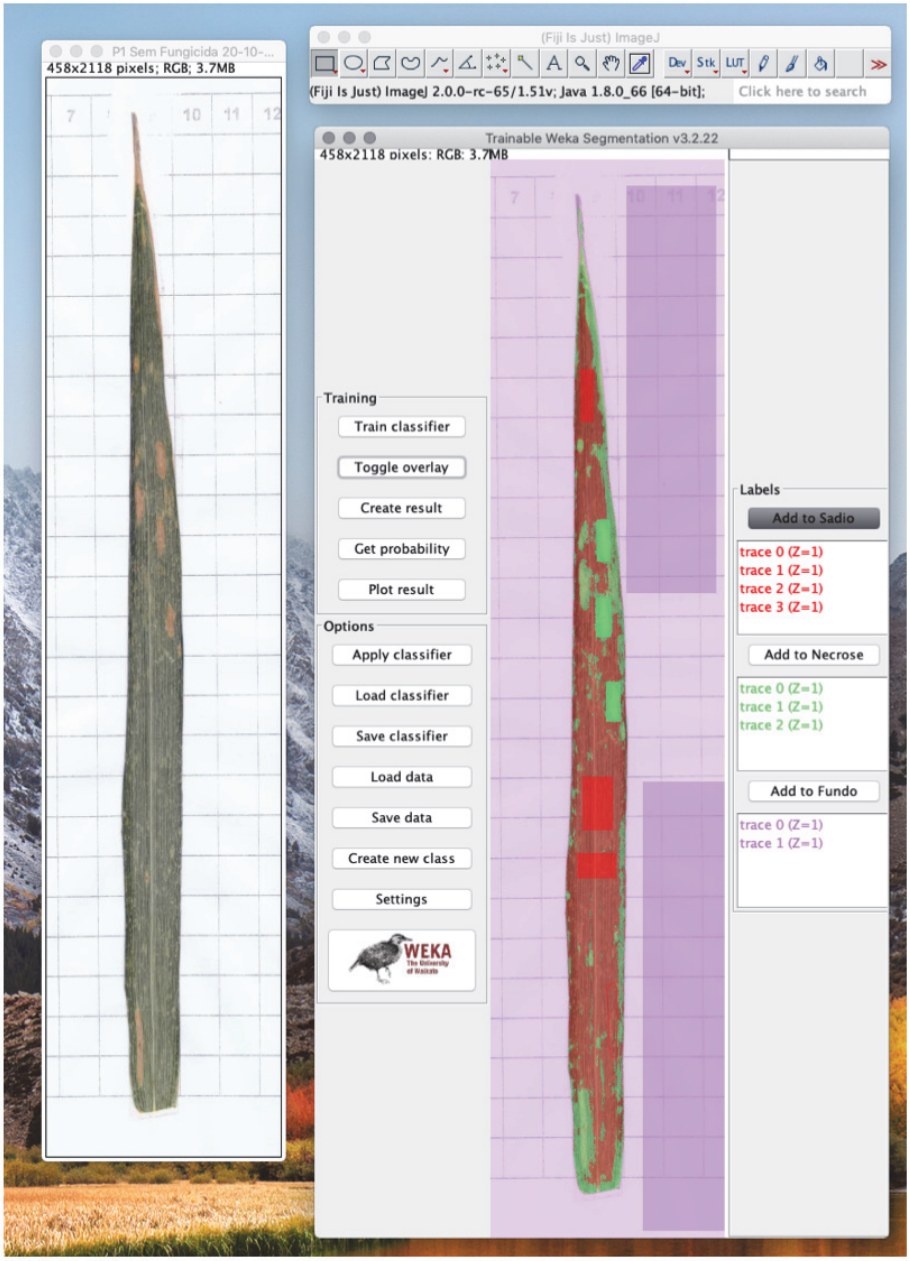

Figure 11. Supervised classification approach for measuring the healthy and necrosis damaged area in wheat leaves.

The supervised classification methodology applied to label and measure damaged area in wheat leaves comprehends three phases: preprocessing, segmentation, and measurement. In the first phase, preprocessing, the image is scaled down to increase the performance of the classification process. Then, the scale of the image is defined by setting the measure in cm corresponding to each pixel. In the segmentation phase, the classifier is applied using the saved model and for each image is generated the probability maps corresponding to each class. Using Otsu [81] global thresholding method for separating pixels into two classes, foreground and background, those probability maps are converted into binary images. Last, from the binary images, the values are obtained: image area (I), background area (BK), necrosis area (N), and healthy area (H). In the measurement phase, the leaf area (L) is calculated subtracting the background area (BK) from the image area (I). Then, necrosis percentual (K) is obtained by K = N/L.

4.4 RESULTS

During the experiment, three different diseases were naturally occuring and affecting the plots simultaneously: powdery mildew, tan spot and fusarium head blight. These diseases were naturally occuring in the wheat field experiments in Coxilha, Rio Grande do Sul, Brazil from 2018 to 2019. During the 2018 field experiment, yellow spots were observed on the plant leaves and grains had a shriveled appearance, symptoms of tan spot and FHB infection, respectively. On the other hand, common signs of powdery mildew infection such as white powdery spots were not observed on the surface of the plants. In 2019, symptoms of the three fungal diseases were observed on the plots however FHB had a mild expression on grain quality loss. Table 4 describes the canopy weight and leaf area observed in each treatment for the two corresponding years.

Table 4. Mean canopy weight and maximum leaf area from the plots with a 7-day, 14-day and 21-day fungicide spraying regimes and control plot with no fungicide application.

Year	Treatment	Canopy Weight (Kg ha$^{-}1$)	Maximum leaf area index (m^2 $m^{-}2$)
2018	7-day interval	15194	5.9
	14-day interval	15688	6.9
	21-day interval	14687	5.9
	No Fungicide	12829	5.0
2019	7-day interval	13079	6.5
	14-day interval	12916	6.0
	21-day interval	12084	5.7
	No Fungicide	11582	6.1

During the simulation, the multiple GDM instances simulated in daily steps the disease cycle of PM, TS and FHB to estimate their respective damage on the wheat crop. The simulated damage was then applied through the pest coupling points to impact the respective state variables. We assumed the spores were present in the field and the spore cloud density was estimated using the data collected by the leaf-wetness sensors 80 cm above ground. The abiotic damage was only applied while having the favorable conditions for infection according to the characteristics of each disease. Powdery mildew and tan spot damage were applied to the leaf area state variable. Fusarium head blight damage was applied to the seed mass state variable. Thus, FHB impacted the seed development when the crop reached the grain filling stage.

In Figure 14, the simulation results for 2018 showed a maximum LAI of 4.2 m^2 m^{-2} across the four treatments. LAI increased rapidly from 46 to 84 days after planting until it reached the maximum LAI. Disease infection started to damage the crop 102 days after planting at the end of ear growth stage, leading to a decrease in LAI up to final harvest date. The simulated scenario with no fungicide application had the biggest reduction on LAI caused by the fungal disease damage. However, considering the mean LAI values of the plots, the model underestimated the LAI for this year. In 2019, all treatments reached a

maximum LAI of 5.3 m^2 m^{-2} at day 83 while pest damage was firstly observed 114 days after planting. For this year, the model had a better performance with a slight underestimation of the maximum LAI.

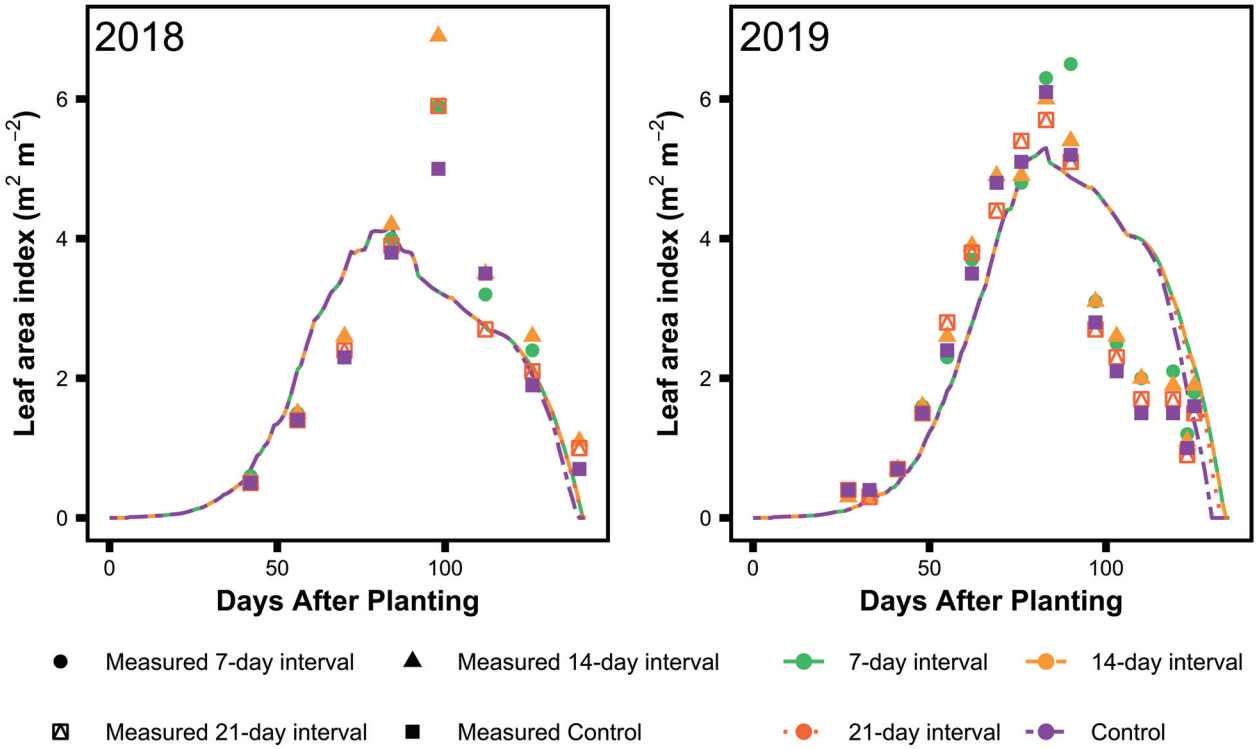

Figure 12. Simulated and measured leaf area index values in 2018 (a) and 2019 (b) for the scenarios with fungicide spraying in intervals of 7-day, 14-day, 21-day and no fungicide application.

The destruction of the leaf area resulted in a shortage of assimilate production, which later in the simulation affected the growth of new leaves. This, consequently, reduced the crop capacity of biomass and yield production. In 2018, the maximum canopy weight of 11417 kg ha^{-1} was observed on the 7-day fungicide spraying regime treatment compared with the lowest yield simulated of 9073 kg ha^{-1} in the no fungicide application treatment. Due to longer periods of lower humidity observed in 2019, the spore cloud density had a significant reduction which led to a lesser severe damage on the wheat crop. In this year the simulated 7-day spraying regime scenario also had the highest canopy weight of 13701 kg ha^{-1} and the no disease control scenario had the lowest canopy weight of 11639 kg ha^{-1} (Figure 13).

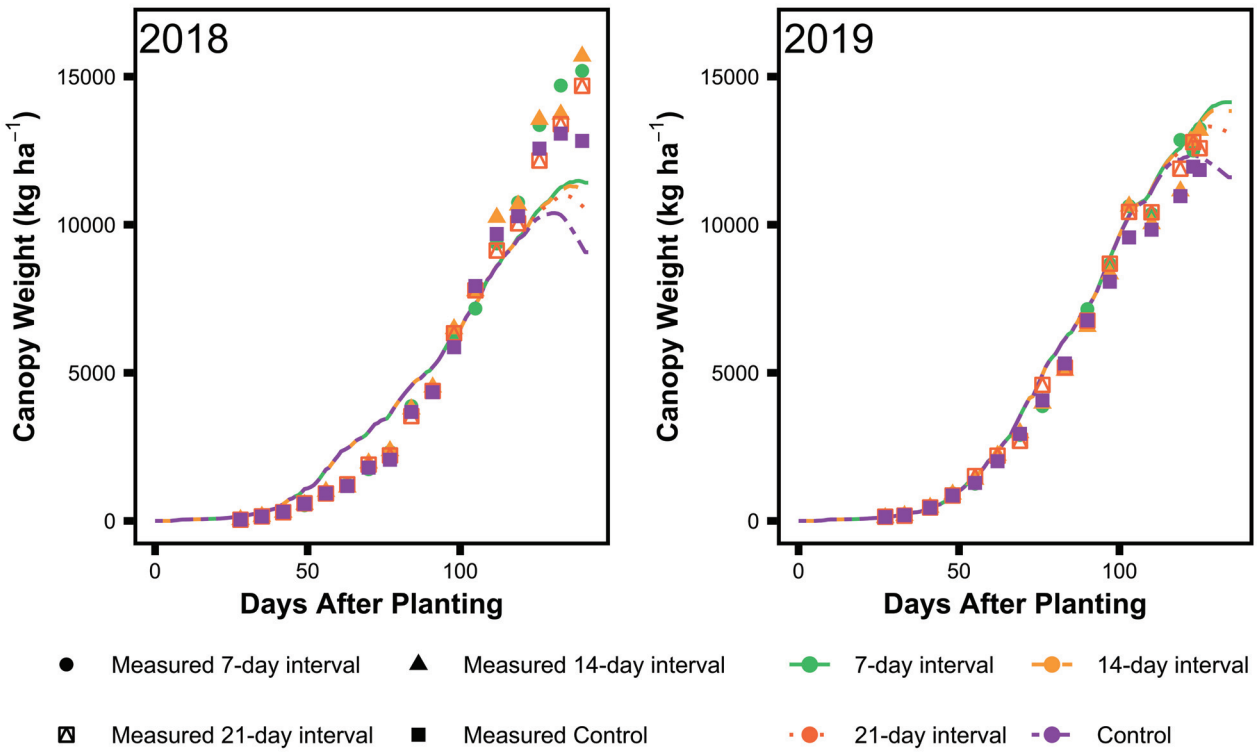

Figure 13. Simulated and measured canopy weight in 2018 (a) and 2019 (b) for the scenarios with fungicide spraying in intervals of 7-day, 14-day, 21-day and no fungicide application.

In 2018, a grain yield of 4405 kg ha^{-1} was observed on the 7-day fungicide spraying regime while the simulated was 4473 kg ha^{-1}. For the 14-day fungicide spraying regime a 4130 kg ha^{-1} grain yield was observed, whereas the model simulated 4174 kg ha^{-1}. For the 21-day fungicide spraying regime was observed a grain yield of 3870 kg ha^{-1} while the simulation estimated 3715 kg ha^{-1}. Regarding the treatment with no fungicide application was observed a yield of 3278 kg ha^{-1}. The model simulated for the same treatment a grain yield of 3121 kg ha^{-1}.

The grain yield in 2019 was, in general, higher than in 2018. In 2019 the observed grain yield was 5041, 4675, 4488 and 4303 kg ha^{-1} respectively for the treatments with fungicide spraying in intervals of 7-day, 14-day, 21-day and no fungicide application. The model simulated for the same treatments grain yield of 5107, 4886, 4499 and 4314 kg ha^{-1} respectively. For both years, the model was capable of simulating canopy weight and yield similarly to the values measured in each treatment. Table 5 details the simulation results outputs for grain yield.

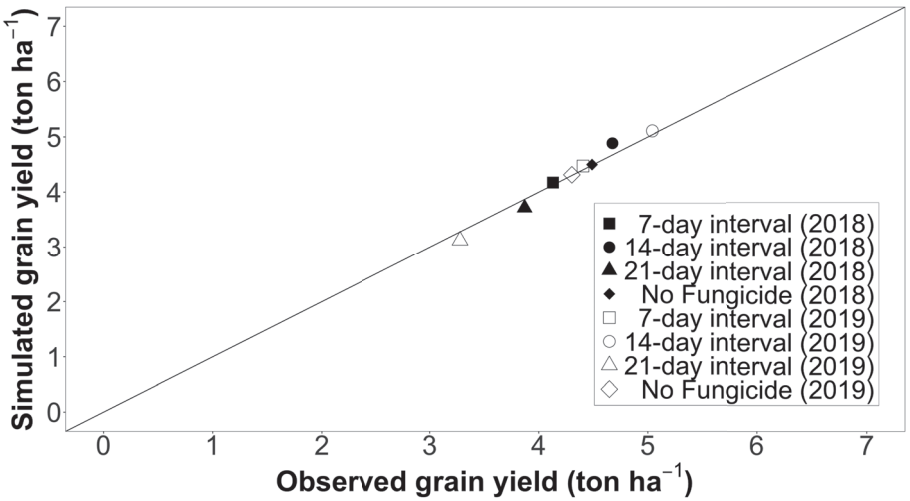

Figure 14. Observed versus simulated grain yields with the coupled DSSAT-NWheat for experiments carried out in Coxilha, RS, Brazil.

4.5 DISCUSSION

One of the objectives of this work was to estimate and combine through a dynamic approach the harmful effects of simultaneous diseases on wheat growth and yield. Most of the wheat agro-physiological models were created primarily to estimate the crop growth disregarding pest and disease impact on crop development and growth processes [18, 56, 58, 19]. Recently pest damage started to be incorporated into these models based on observed data and simple mechanistic approaches [15, 17]. The disease models used in this study were designed and parameterized to mimic the cycle of fungal diseases based on cohorts [82] and estimate the damaging effects on wheat crops. Through the MPI interface, the wheat crop growth model and the disease models were coupled into a complex structure (Figure 9). The exchange of messages between models, without modifying the wheat model source code, allowed the communication among those models during execution.

The case studies have shown how this multiple model approach is capable of simulating pest and disease damage. The biotic stress of powdery mildew and tan spot impacted the leaf area index and, consequently, the crop yield while FHB reduced the crop grain mass. Besides the disease cycle, the disease models also considered during the simulation several factors such as cultivar resistance and infection efficiency. For both years, the modified model simulated correctly grain yield. A more severe damage on yield was measured and simulated for 2018 (Table 5) which is likely due to the longer periods of high humidity and precipitation which provided more favorable conditions for fungal infection. Canopy weight value was also well simulated in 2019 and slightly underestimated in 2018 by the model. However, the LAI pattern observed was underestimated for both years, especially in 2018. The CSM-NWheat model did not estimate a LAI growth as observed which may be correlated to the model tendency to underestimate the crop LAI production [19]. Overall, the response of this coupling approach nevertheless appears to be reliable with respect to this

evaluation phase. The resulting yield loss was comparable with the measured data showing the capability of the model for simulating the FHB, PM, and TS diseases.

Results of this work also illustrate the capability of connecting a wheat model to communicate with multiple independent diseases models through a MPI interface. The modified model can now estimate the impact on crop growth and yield. The simulated inoculum on this research did not take into account externally originated spores due to the complexity of estimating spore production outside the simulation environment. Different scenarios of initial inoculum density could be further explored using this approach. More testing should be performed to determine if the developed method can properly estimate the effect of these diseases on other regions with different soil properties, environment conditions and fertilizer application regimes.

4.6 CONCLUSION

This work provides a multi-model approach for simulating the damage effect of powdery mildew (*Blumeria graminis f. sp. tritici*), tan spot (*Pyrenophora tritici-repentis*) and fusarium head blight (*Gibberella zeae*). Each disease was simulated using independent models, driven by factors associated with the pathogen and environmental conditions. A MPI Interface allowed the communication between the wheat crop model and the disease models. The data exchange among these models were given in daily steps for which the CSM-NWheat broadcasted the daily leaf area and seed mass while the disease models estimated the infection and damage rates. These disease damage rates were communicated to the selected disease coupling point inside the crop growth model to reduce the leaf area or seed mass state variables. Powdery mildew and tan spot damage impacted the simulated wheat leaf area and, consequently, had an effect on grain production. Fusarium head blight damage was applied at the grain filling stage to impact the daily seed mass, reducing the wheat grain yield. The multi-model approach presented in this work was tested successfully using field experiments in Brazil. The results demonstrated the coupled model's capability to simulate the fungal infection damage on crop growth and, specially, yield. The method described can be used in future studies as a decision support system for simulating the impact of powdery mildew, tan spot and fusarium head blight or, an example for coupling distinct models to simulate the effects of pests and diseases on wheat crops.

5. CONCLUSION AND FUTURE WORK

Coupling pests and diseases models with crop growth models is a major step to produce more precise simulations under real farm conditions. This work extended the use of pest and disease models and developed a multi-model approach to estimate the effects of several pests on grain yield. The communication approach demonstrated capability to link three disease models and predict crop response to wheat blast infection in multiple locations. This is the first empirical study to use a multi-model approach able to predict the impact of pests on wheat yield. This will extend the use of crop models in conjunction with disease models to comprehend a broad range of problems often seen in the real world. The final objective of this work was to help improve the predictions of production and assist on the decision making. The technology used in this study proves to be the potential for collaborative work within the crop modeling community.

The communication structure has potential to couple DSSAT crop models to other disease models. Besides, fungal diseases such as rice blast have similar characteristics and behaviors as *Magnaporthe oryzae triticum* [83]. Thus, this approach can also simulate fungal diseases in different crops with adjustments in the disease parameters. Future work is planned to develop the coupling point to the CERES-Rice [58], a rice simulation model within the Cropping System Model of DSSAT, with pest and disease models and estimate the effects of rice blast [84] on crop growth and development. Additionally, the use of hourly data of relative humidity may also improve the simulation results of this work.

This work can also be applied for simulating in a regional or even global scale the impact of several pests and pathogens on wheat. This would include measuring its performance in other regions and climates. Through the use of forecast weather data it is possible to simulate several future scenarios and help improve decision making by identifying an appropriate time-window for fungicide application. This could also work in conjunction with integrated pest control techniques to assist on crop management of wheat fields. The technology used in this study proves to be potential for collaborative work within the crop modeling community allowing researchers to simulate the interactions of pests and diseases with wheat growth.

REFERENCES

[1] BRAUN, H.-J. et al. Multi-location testing as a tool to identify plant response to global climate change. *Climate change and crop production*, CABI Wallingford, UK, v. 1, p. 115–138, 2010.

[2] SAVARY, S. et al. The global burden of pathogens and pests on major food crops. *Nature ecology & evolution*, Nature Publishing Group, v. 3, n. 3, p. 430, 2019.

[3] SAVARY, S. et al. Quantification and modeling of crop losses: a review of purposes. *Annu. Rev. Phytopathol.*, Annual reviews, v. 44, p. 89–112, 2006.

[4] WHISH, J. P. et al. Integrating pest population models with biophysical crop models to better represent the farming system. *Environmental Modelling & Software*, Elsevier, v. 72, p. 418–425, 2015.

[5] DONATELLI, M. et al. Modelling the impacts of pests and diseases on agricultural systems. *Agricultural systems*, Elsevier, v. 155, p. 213–224, 2017.

[6] WIT, C. D.; VRIES, F. P. de. La synthese et la simulation des systemes de production primaire. In: *La productivite des paturages Saheliens*. [S.l.]: Pudoc, 1982. p. 23–27.

[7] SPITTERS, C. Crop growth models: their usefulness and limitations. In: *VI Symposium on the Timing of Field Production of Vegetables 267*. [S.l.: s.n.], 1989. p. 349–368.

[8] WILKERSON, G. et al. Modeling soybean growth for crop management. *Transactions of the ASAE*, American Society of Agricultural and Biological Engineers, v. 26, n. 1, p. 63–0073, 1983.

[9] WILKERSON, G. et al. Sicm florida soybean integrated crop management model: Model description user's guide. *Agr. Eng. Dep. Rpt. AGE*, p. 83–1, 1983.

[10] BOOTE, K. et al. Coupling pests to crop growth simulators to predict yield reductions [mathematical models]. *Phytopathology (USA)*, 1983.

[11] JONES, J. et al. Integration of soybean crop and pest models. In: *Symposium sponsored by the Consortium for Integrated Pest Management and USDA/CSRS*. [S.l.: s.n.], 1985.

[12] BATCHELOR, W. et al. Extending the use of crop models to study pest damage. *Transactions of the ASAE*, American Society of Agricultural and Biological Engineers, v. 36, n. 2, p. 551–558, 1993.

[13] PINNSCHMIDT, H.; BATCHELOR, W.; TENG, P. Simulation of multiple species pest damage in rice using ceres-rice. *Agricultural Systems*, Elsevier, v. 48, n. 2, p. 193–222, 1995.

[14] HOOGENBOOM, G. et al. The dssat crop modeling ecosystem. In: BOOTE, K. (Ed.). *Advances in Crop Modeling for a Sustainable Agriculture*. Cambridge, United Kingdom: Burleigh Dodds Science Publishing, 2019. p. 173–216.

[15] WILLOCQUET, L. et al. Simulating multiple pest damage in varying winter wheat production situations. *Field Crops Research*, Elsevier, v. 107, n. 1, p. 12–28, 2008.

[16] MAGAREY, R.; SUTTON, T.; THAYER, C. A simple generic infection model for foliar fungal plant pathogens. *Phytopathology*, Am Phytopath Society, v. 95, n. 1, p. 92–100, 2005.

[17] RÖLL, G. et al. Development and evaluation of a leaf disease damage extension in cropsim-ceres wheat. *Agronomy*, Multidisciplinary Digital Publishing Institute, v. 9, n. 3, p. 120, 2019.

[18] HUNT, L.; PARARAJASINGHAM, S. Cropsim—wheat: A model describing the growth and development of wheat. *Canadian Journal of Plant Science*, NRC Research Press Ottawa, Canada, v. 75, n. 3, p. 619–632, 1995.

[19] KASSIE, B. T. et al. Performance of dssat-nwheat across a wide range of current and future growing conditions. *European Journal of Agronomy*, Elsevier, v. 81, p. 27–36, 2016.

[20] CILAS, C. et al. Tropical crop pests and diseases in a climate change setting—a few examples. In: *Climate change and agriculture worldwide*. [S.l.]: Springer, 2016. p. 73–82.

[21] ISLAM, M. T.; KIM, K.-H.; CHOI, J. Wheat blast in bangladesh: the current situation and future impacts. *The plant pathology journal*, The Korean Society of Plant Pathology, v. 35, n. 1, p. 1, 2019.

[22] FERNANDES, J. M. C. et al. A weather-based model for predicting early season inoculum build-up and spike infection by the wheat blast pathogen. *Tropical plant pathology*, Springer, v. 42, n. 3, p. 230–237, 2017.

[23] EBBOLE, D. J. Magnaporthe as a model for understanding host-pathogen interactions. *Annu. Rev. Phytopathol.*, Annual Reviews, v. 45, p. 437–456, 2007.

[24] WILSON, R. A.; TALBOT, N. J. Under pressure: investigating the biology of plant infection by magnaporthe oryzae. *Nature Reviews Microbiology*, Nature Publishing Group, v. 7, n. 3, p. 185–195, 2009.

[25] TRAIL, F. For blighted waves of grain: Fusarium graminearum in the postgenomics era. *Plant physiology*, Am Soc Plant Biol, v. 149, n. 1, p. 103–110, 2009.

[26] PESTKA, J. J. Deoxynivalenol: toxicity, mechanisms and animal health risks. *Animal feed science and technology*, Elsevier, v. 137, n. 3-4, p. 283–298, 2007.

[27] ALVI, A. H. et al. Field evolved resistance in helicoverpa armigera (lepidoptera: Noctuidae) to bacillus thuringiensis toxin cry1ac in pakistan. *PLoS One*, Public Library of Science, v. 7, n. 10, p. e47309, 2012.

[28] SINGH, R. P. et al. Disease impact on wheat yield potential and prospects of genetic control. *Annual Review of Phytopathology*, v. 54, n. 1, p. 303–322, 2016. PMID: 27296137.

[29] MALAKER, P. K. et al. First report of wheat blast caused by magnaporthe oryzae pathotype triticum in bangladesh. American Phytopathological Society (APS), 2016.

[30] CERESINI, P. C. et al. Wheat blast: past, present, and future. *Annual Review of Phytopathology*, Annual Reviews, 2018.

[31] GLAWE, D. A. The powdery mildews: a review of the world's most familiar (yet poorly known) plant pathogens. *Annual review of phytopathology*, v. 46, 2008.

[32] SCHIERENBECK, M. et al. Combinations of fungicide molecules and nitrogen fertilization revert nitrogen yield reductions generated by pyrenophora tritici-repentis infections in bread wheat. *Crop Protection*, Elsevier, v. 121, p. 173–181, 2019.

[33] MCINTOSH, R. et al. Catalogue of gene symbols for wheat. In: SASKATOON: PRINT CRAFTERS. *Proc. 9th Int. Wheat Genet. Symp*. [S.l.], 1998. v. 5, p. 1–235.

[34] KEATING, B. A. et al. An overview of apsim, a model designed for farming systems simulation. *European journal of agronomy*, Elsevier, v. 18, n. 3-4, p. 267–288, 2003.

[35] HOLZWORTH, D. et al. Apsim next generation: Overcoming challenges in modernising a farming systems model. *Environmental Modelling & Software*, Elsevier, v. 103, p. 43–51, 2018.

[36] JONES, J. W. et al. The dssat cropping system model. *European journal of agronomy*, Elsevier, v. 18, n. 3-4, p. 235–265, 2003.

[37] BOOTE, K. et al. The cropgro model for grain legumes. In: *Understanding options for agricultural production*. [S.l.]: Springer, 1998. p. 99–128.

[38] G., H. et al. *Decision Support System for Agrotechnology Transfer Version 4.5. Volume 1: Overview*. University of Hawaii, Honolulu, HI: [s.n.], 2010. ISBN 1886684065.

[39] W.D., B. et al. *Decision Support System for Agrotechnology Transfer Version 4.5. Volume 4. DSSAT v4.5: Crop Model Documentation. Chapter 13: Pest and Disease Damage Module*. University of Hawaii, Honolulu, HI: [s.n.], 2010. 353-403 p. ISBN 1886684081.

[40] FRAZER, B.; GILBERT, N. et al. Coccinellids and aphids: a quantitative study of the impact of adult ladybirds (coleoptera: Coccinellidae) preying on field populations of pea aphids (homoptera: Aphididae). *Journal of the Entomological Society of British Columbia*, v. 73, p. 33–56, 1976.

[41] W., J. J. et al. *Decision Support System for Agrotechnology Transfer Version 4.0. Volume 4. DSSAT v4.5: Crop Model Documentation*. University of Hawaii, Honolulu, HI: [s.n.], 2005. 353–403 p. ISBN 1886684081.

[42] SAVARY, S. et al. Modelling and mapping potential epidemics of wheat diseases—examples on leaf rust and septoria tritici blotch using epiwheat. *European journal of plant pathology*, Springer, v. 142, n. 4, p. 771–790, 2015.

[43] CAUBEL, J. et al. Climate change effects on leaf rust of wheat: Implementing a coupled crop-disease model in a french regional application. *European Journal of Agronomy*, Elsevier, v. 90, p. 53–66, 2017.

[44] BRISSON, N. et al. An overview of the crop model stics. *European Journal of agronomy*, Elsevier, v. 18, n. 3-4, p. 309–332, 2003.

[45] PRANK, M. et al. Climate change impacts the spread potential of wheat stem rust, a significant crop disease. *Environmental Research Letters*, IOP Publishing, v. 14, n. 12, p. 124053, 2019.

[46] BREGAGLIO, S. et al. Comparing process-based wheat growth models in their simulation of yield losses caused by plant diseases. *Field Crops Research*, Elsevier, v. 265, p. 108108, 2021.

[47] PAVAN, W.; FERNANDES, J. M. C. Uso de orientação a objetos no desenvolvimento de modelos de simulação de doenças de plantas genéricos. *Revista Brasileira de Agroinformática*, v. 9, n. 1, p. 12–27, 2009.

[48] FERNANDES, J. et al. Improving crop pest/disease modeling. *Embrapa Trigo-Capítulo em livro científico (ALICE)*, In: BOOTE, K.(Ed.). Advances in crop modelling for a sustainable agriculture . . . , 2019.

[49] BERGER, R.; JONES, J. A general model for disease progress with functions for variable latency and lesion expansion on growing host plants. *Phytopathology*, American Phytopathological Society, v. 75, n. 7, p. 792–797, 1985.

[50] BERGER, R. et al. A simulation model to describe epidemics of rust of phaseolus beans i. development of the model and sensitivity analysis. *Phytopathology*, [St. Paul, Minn., etc.: American Phytopathological Society], v. 85, n. 6, p. 715–721, 1995.

[51] WILLOCQUET, L.; SAVARY, S. An epidemiological simulation model with three scales of spatial hierarchy. *Phytopathology*, Am Phytopath Society, v. 94, n. 8, p. 883–891, 2004.

[52] OERKE, E. Crop losses to pests. *The Journal of Agricultural Science*, Cambridge University Press, v. 144, p. 31, 2006.

[53] FAROOK, U. B. et al. A review on insect pest complex of wheat (triticum aestivum l.). *Journal of Entomology and Zoology Studies, 7 (1)*, p. 1292–1298, 2019.

[54] SHEWRY, P. R. Wheat. *Journal of experimental botany*, Oxford University Press, v. 60, n. 6, p. 1537–1553, 2009.

[55] WEST, P. C. et al. Leverage points for improving global food security and the environment. *Science*, American Association for the Advancement of Science, v. 345, n. 6194, p. 325–328, 2014.

[56] BOOGAARD, H. et al. *WOFOST 7.1; user's guide for the WOFOST 7.1 crop growth simulation model and WOFOST Control Center 1.5*. [S.l.], 1998.

[57] TSUJI, G. Y.; HOOGENBOOM, G.; THORNTON, P. K. *Understanding options for agricultural production*. [S.l.]: Springer Science & Business Media, 1998. v. 7.

[58] RITCHIE, J. et al. Cereal growth, development and yield. In: *Understanding options for agricultural production*. [S.l.]: Springer, 1998. p. 79–98.

[59] BOOTE, K. J. et al. The role of crop systems simulation in agriculture and environment. *International Journal of Agricultural and Environmental Information Systems (IJAEIS)*, IGI Global, v. 1, n. 1, p. 41–54, 2010.

[60] BOOTE, K. et al. *Advances in crop modelling for a sustainable agriculture.* [S.l.]: Burleigh Dodds Science Publishing Limited, 2020.

[61] WILKERSON, G. et al. Florida soybean integrated crop management model: Model description and user's guide. In: *Unpublished report prepared for the Soybean Consortium for Integrated Pest Management Modeling Workshop, Univ. Florida, Gainesville, Florida*. [S.l.: s.n.], 1982. p. 22–25.

[62] BOOTE, K. et al. *Pnutgro V1.02: Peanut Crop Growth Simulation Model : User's Guide*. University of Florida, Department of Agricultural Engineering, 1989. (Florida Agricultural Experiment Station journal). Disponível em: <https://books.google.com.br/books?id=uknFHAAACAAJ>.

[63] BATCHELOR, W. D. et al. Simulation of maize lethal necrosis (mln) damage using the ceres-maize model. *Agronomy*, Multidisciplinary Digital Publishing Institute, v. 10, n. 5, p. 710, 2020.

[64] FIGUEROA, M.; HAMMOND-KOSACK, K. E.; SOLOMON, P. S. A review of wheat diseases—a field perspective. *Molecular plant pathology*, Wiley Online Library, v. 19, n. 6, p. 1523–1536, 2018.

[65] TENG, P. et al. Simulation of pest effects on crops using coupled pest-crop models: the potential for decision support. In: *Understanding options for agricultural production*. [S.l.]: Springer, 1998. p. 221–266.

[66] HALL, M. et al. The weka data mining software: an update. *ACM SIGKDD explorations newsletter*, ACM New York, NY, USA, v. 11, n. 1, p. 10–18, 2009.

[67] BOURAS, N.; KIM, Y. M.; STRELKOV, S. E. Influence of water activity and temperature on growth and mycotoxin production by isolates of pyrenophora tritici-repentis from wheat. *International journal of food microbiology*, Elsevier, v. 131, n. 2-3, p. 251–255, 2009.

[68] SINGH, P. et al. Genetics of wheat–pyrenophora tritici-repentis interactions. *Euphytica*, Springer, v. 171, n. 1, p. 1–13, 2010.

[69] SHEWRY, P. R.; HEY, S. J. The contribution of wheat to human diet and health. *Food and energy security*, Wiley Online Library, v. 4, n. 3, p. 178–202, 2015.

[70] RABBINGE, R.; RIJSDIJK, F. Disease and crop physiology: a modeller's point of view. In: *Effects of Disease on the Physiology of the Growing Plant*. [S.l.]: CUP, 1982. p. 201–220.

[71] MEMIC, E. et al. Extending the csm-ceres-beet model to simulate impact of observed leaf disease damage on sugar beet yield. *Agronomy*, Multidisciplinary Digital Publishing Institute, v. 10, n. 12, p. 1930, 2020.

[72] FERREIRA, T. et al. Coupling a pest and disease module with a wheat crop simulation model. *Unpublished*.

[73] PAYROS, D. et al. Toxicology of deoxynivalenol and its acetylated and modified forms. *Archives of toxicology*, Springer, v. 90, n. 12, p. 2931–2957, 2016.

[74] PONTE, E. M. D. et al. A model-based assessment of the impacts of climate variability on fusarium head blight seasonal risk in southern brazil. *Journal of Phytopathology*, Wiley Online Library, v. 157, n. 11-12, p. 675–681, 2009.

[75] GABRIEL, E. et al. Open mpi: Goals, concept, and design of a next generation mpi implementation. In: SPRINGER. *European Parallel Virtual Machine/Message Passing Interface Users' Group Meeting*. [S.l.], 2004. p. 97–104.

[76] BROWNE, P. A.; WILSON, S. A simple method for integrating a complex model into an ensemble data assimilation system using mpi. *Environmental Modelling & Software*, Elsevier, v. 68, p. 122–128, 2015.

[77] ALVARES, C. A. et al. Koppen's climate classification map for brazil. *Meteorologische Zeitschrift*, Stuttgart, v. 22, n. 6, p. 711–728, 2013.

[78] STRECK, E. et al. Solos do rio grande do sul. *Environmental Modelling & Software*, Porto Alegre: Emater-RS / Ascar, 2008., v. 2, p. 222, 2008.

[79] ZADOKS, J. C. et al. A decimal code for the growth stages of cereals. *Weed research*, v. 14, n. 6, p. 415–421, 1974.

[80] SCHINDELIN, J. et al. Fiji: an open-source platform for biological-image analysis. *Nature methods*, Nature Publishing Group, v. 9, n. 7, p. 676–682, 2012.

[81] OTSU, N. A threshold selection method from gray-level histograms. *IEEE transactions on systems, man, and cybernetics*, IEEE, v. 9, n. 1, p. 62–66, 1979.

[82] BERGER, R. Description and application of some general models for plant disease epidemics. In: LEONARD, K. J.; FRY, W. E. (Ed.). [S.l.]: Kluwer Academic Publishers, 1989. v. 2, n. 7, p. 125–149.

[83] PONTE, E. M. D.; VALENT, B.; BERGSTROM, G. C. A special issue on fusarium head blight and wheat blast. *Tropical Plant Pathology*, Springer, v. 42, n. 3, p. 143–145, 2017.

[84] SHAHRIAR, S. A. et al. Rice blast disease. *Annual Research & Review in Biology*, p. 50–64, 2020.

ATTACHMENT A – APPENDIX

The following is the CSM-NWheat source code to estimate pest and disease damage effect on crop growth:

```
LAIDOT = 0
IF (PLTPOP .GT. 0.0 .AND. plantwt(leaf_part) .GT. 0.0 .AND. WLIDOT .GT. 0.0) THEN
   LAIDOT = WLIDOT * ((pl_la - sen_la) /100) / (plantwt(leaf_part))
ENDIF

IF(PLTPOP.GT.0.0) THEN
    pl_nit(leaf_part) = pl_nit (leaf_part) -
&   pl_nit(leaf_part) * (WLIDOT/PLTPOP) / plantwt(leaf_part)
    plantwt(leaf_part) = plantwt(leaf_part) - WLIDOT/PLTPOP
    plantwt(leaf_part) = MAX(plantwt(leaf_part),0.0)
ENDIF
    pl_la = pl_la - (LAIDOT * 100/PLTPOP)
    LAI = LAI - LAIDOT/10000
    LAI = MAX(LAI, 0.0)
```

Figure 15. Source code to apply daily pest and disease damage to LAI and leaf mass.

```
IF(PLTPOP.GT.0.0 .AND. plantwt(stem_part) .GT. 0.0 .AND. WSIDOT .GT. 0.0) THEN
    pl_nit(stem_part)=pl_nit(stem_part) - pl_nit(stem_part)*(WSIDOT/PLTPOP)/plantwt(stem_part)
    plantwt(stem_part) = plantwt(stem_part) - WSIDOT/PLTPOP
    plantwt(stem_part) = MAX(plantwt(stem_part), 0.0)
ENDIF
```

Figure 16. Source code to apply daily pest and disease damage to stem mass.

```
IF(PLTPOP.GT.0.0 .AND. plantwt(root_part) .GT. 0.0 .AND. WRIDOT .GT. 0.0) THEN
    pl_nit(root_part)= pl_nit(root_part) - pl_nit(root_part)*(WRIDOT/PLTPOP)/plantwt(root_part)
    plantwt(root_part) = plantwt(root_part) - WRIDOT/PLTPOP
    plantwt(root_part) = MAX(plantwt(root_part), 0.0)
ENDIF
```

Figure 17. Source code to apply daily pest and disease damage to root mass.

```
IF (PLTPOP.GT. 0.0 .AND. plantwt(grain_part) .GT. 0.0 .AND.
&   SWIDOT .GT. 0.0) THEN
    pl_nit(grain_part) = pl_nit(grain_part) - pl_nit(grain_part)*
&  (SWIDOT/PLTPOP)/plantwt(grain_part)
    gpp = gpp - gpp *(SWIDOT/PLTPOP)/plantwt(grain_part)
ENDIF

IF(PLTPOP.GT.0.0 .AND. SWIDOT .GT. 0.0) THEN
    plantwt(grain_part) = plantwt(grain_part) - SWIDOT/PLTPOP
    plantwt(grain_part) = MAX(plantwt(grain_part), 0.0)
    plantwt(seed_part) = plantwt(seed_part) - SWIDOT/PLTPOP
    plantwt(seed_part) = MAX(plantwt(seed_part), 0.0)
ENDIF
```

Figure 18. Source code to apply daily pest and disease damage to seed mass.

```
LAI = (pl_la - sen_la)
AREALF = LAI * 10000
AREAH  = AREALF - DISLA
AREAH  = MAX(0.,AREAH)
XHLAI = AREAH/10000
radfr = 1.0 - exp (-nwheats_kvalue * XHLAI)
```

Figure 19. Source code to simulate leaf area necrosis and apply daily damage to the healthy leaf area.

```
pcarbo = pcarbo - ASMDOT
pcarbo = MAX(pcarbo, 0.0)
```

Figure 20. Source code to apply daily pest and disease damage and reduce the potential dry matter production.

```
1  IF(PLTPOP.GT. 0.0 .AND. PPLTD.GT.0) THEN
2      PLTPOP = PLTPOP - PLTPOP * PPLTD/100
3      PLTPOP = MAX(PLTPOP, 0.0)
4      LAI = LAI - LAI*(PPLTD/100)
5      LAI = MAX(LAI, 0.0)
6  ENDIF
```

Figure 21. Source code to apply daily pest and disease damage that affects all plant parts.

UPF
UNIVERSIDADE
DE PASSO FUNDO

UPF Campus I - BR 285, São José
Passo Fundo - RS - CEP: 99052-900
(54) 3316 7000 - www.upf.br